論文 / 著書情報
Article / Book Information

題目(和文)	筋活動に基づく人間の感覚・運動適応に関する研究
Title(English)	The study of human sensory motor adaptation in terms of muscle activation
著者(和文)	
Author(English)	Edwardo Arata Yamamo Murakami
出典(和文)	学位:博士(学術), 学位授与機関:東京工業大学, 報告番号:甲第8842号, 授与年月日:2012年3月26日, 学位の種別:課程博士, 審査員:小池 康晴
Citation(English)	Degree:Doctor (Academic), Conferring organization: Tokyo Institute of Technology, Report number:甲第8842号, Conferred date:2012/3/26, Degree Type:Course doctor, Examiner:
学位種別(和文)	博士論文
Type(English)	Doctoral Thesis

The study of human sensory motor adaptation in terms of muscle activation

by

Edwardo Arata Yamamoto Murakami

Submitted to the Department of Computer Intelligence and Systems Science
in partial fulfillment of the requirements for the degree of

Doctor of Philosophy

at the

TOKYO INSTITUTE OF TECHNOLOGY

March 2012

Author .....
Department of Computer Intelligence and Systems Science
March, 2012

Certified by .....
Yasuharu Koike
Professor
Thesis Supervisor

The study of human sensory motor adaptation in terms of muscle activation

by

Edwardo Arata Yamamoto Murakami

Submitted to the Department of Computer Intelligence and Systems Science
on March, 2012, in partial fulfillment of the
requirements for the degree of
Doctor of Philosophy

Abstract

First, an introduction about the motivation and the purpose of this research is given. In the second chapter a general overview about the human motor learning is introduced focused on both upper and lower limbs studies. In the third chapter the measurement about the human reaction time related to visual and force feedback is described and compared with the response time estimated from a continuous pursuit control task. It was shown that the human acquired model depended on the machine characteristics and the learned model was associated with the transfer function order. When different sensorial information was available to the subjects, there were noted small variations in the transfer function parameters representing the subject's capability to adapt to different sensorial feedback information. The chapter 4 described the EMG and ground reaction force (GRF) measurements in order to analyze the effects of toe movement during gait and running. All the subjects performed 4 different trial modes. When a significant difference between the barefoot and shod walk/run was observed, the EMG activity of shod walk/run was smaller. The toe movement showed no statistical difference compared to normal walk/run in shod trials. The human motor learning was represented by a statistical difference between the trial modes and the motor adaptation occurred when no difference was verified. In the walking and running experiment it was observed from the GRF profiles that the toe movement showed to be a potential way of changing in an active manner the characteristics of shock absorption. In the fifth chapter the two approaches chosen in this study to analyze the motor learning and adaptation are discussed. Finally, this study described quantitatively how to differentiate the human sensory motor learning and adaptation related to pursuit control tasks and walk/run analysis in order to apply it in the design and evaluation of sports gear and everyday life tools.

論文要旨 (Abstract in Japanese)

本論文は「The study of human sensory motor adaptation in terms of muscle activation (筋活動に基づく人間の感覚・運動適応に関する研究)」と題し，英文で6章より構成されている．

第1章「INTRODUCTION（はじめに）」では，本研究の目的が，上肢と下肢動作の運動学や運動力学特徴に加えて筋電信号も計測し解析を行うことで，人間の運動制御と感覚系における学習・適応メカニズムを調べることであると述べている．

第2章「MOTOR CONTROL LEARNING（人間の運動学習）」では，人間の運動制御に関するこれまでの研究を学習と適応に焦点をあて，人間がどのように新しい運動を学習し，身体を制御して新たな環境に適応するかについて概説している．

第3章「HUMAN CONTROL MODEL BASED ON SENSORY FEEDBACK INFORMATION（感覚フィードバック情報に基づく人間の制御モデル)」では，人間の反応時間を直接計測し，筋骨格系による生理的特性や知覚認識による判断遅れについてデータを解析している．その結果，生理的特性として視覚刺激が提示されてから約80-120msで運動指令が筋肉に伝達され，それから約150msで回転動作が開始されることがわかったと述べている．さらに，制御特性として，判断が必要な場合は約40-80msの時間が追加されると述べている．前記で求めた反応時間を参考に，視覚追従実験に加えて力制御実験に基づく制御動作実験を行っている．マスタのダイヤルを操作してスレーブのリニアアクチュエータで駆動されるスライダを制御する3つの実験を行い，それぞれの操作者制御モデルを同定した結果，従来研究の知見と同様に人間・機械系の一巡伝達特性が交差周波数付近では1次遅れに近い特徴を示すことを確認している．さらに，シーソーを操作する実験では操作者が微分動作，つまり制御対象を予測できる要素を獲得できること，また，力覚情報を付加することによって腕のインピーダンスが増し，比例動作が増加することを示している．これにより，被験者間では時定数と反応時間に顕著な差が生じ，個人差を表現できると述べている．

第4章「EFFECTS OF TOE MOVEMENT DURING WALKING AND RUNNING IN TERMS OF GRF AND EMG SIGNALS（歩行・走行時の足部MP関節の動きにおける床反力と筋電計測)」では，裸足またはシューズを使用時，さらに足の指先(MP関節)を屈曲または通常の場合の計4種類の歩行・走行動作の計測に加え床反力および下腿の筋電信号を計測し，被験者毎の特性を比較検討している．踵接地瞬間(HC)を基準に3つの区間(Before HC, Around HC, After HC)における足部の屈筋と伸筋の筋電信号を比較した結果，時間的変化の特徴は被験者間で大きく異なるが，共通してシューズ使用時に筋活動が小さくなると述べている．また，MP関節を屈曲または通常の歩行・走行の間で，筋活動に有意な差が存在したのは裸足のときのみであったことを確認している．

第5章「HUMAN MOTOR LEARNING AND ADAPTATION（運動学習と適応)」では，第3章，4章の実験結果から，運動学習と適応の関係を明らかにしている．反応時間計測実験では主に知覚認知部分における判断時間が被験者によって異なっているが，この特徴は制御動作実験においても引き続き観察されることを指摘している．また，制御パラメータは被験者によって異なっていたが，機械の特性に合わせて自らの制御伝達特性を変化させていることを見いだしている．これらのことから，人間の制御モデルを伝達関数の形で表現することによって学習と適応の違いについて述べている．歩行・走行実験では，被験者毎の運動学習適応パターンの違いを筋電信号

の違いから説明している.

第6章「CONCLUSION（まとめ）」では，反応計測実験と歩行・走行実験における運動の学習や適応の違いを筋電信号により定量的に評価する手法が，将来新たに設計する製品の評価に応用可能であることを述べている.

Thesis Supervisor: Yasuharu Koike
Title: Professor

Acknowledgments

I am greatly indebted to my thesis supervisor Professor Dr. Yasuharu Koike for providing me with definite direction, professional guidance and constant encouragement from the beginning of the work and moral support in many ways during my PhD course period.

I am also greatly indebted to Prof. Makoto Sato, Prof. Yoshihiro Miyake, Prof. Hiroshi Nagahashi and Prof. Osamu Hasegawa, of Tokyo Institute of Technology, for their valuable suggestion and direction to accomplish the study.

I am very grateful for all the support and understanding of Dr. Toshihiro Matsui, Deputy Director General of the Information Technology and Electronics Dept. (AIST), who gave me the opportunity to continue my research at Digital Human Research Center (DHRC).

I acknowledge the help, advice and guidance rendered by the former Director of Digital Human Research Center, Dr. Takeo Kanade and Dr. Masaaki Mochimaru, the present Director.

I am also grateful to all the colleagues of the Digital Human Research Center.

I am very grateful for all the support of Samsung Yokohama Research Institute.

I am also grateful to all members of Koike Laboratory.

I would like to thank Mizuno Corporation for supporting part of this work.

I would like to express my sincere thanks to late Mr. Masanori Honjo, founder of ITO EN, LTD. and Honjo International Scholarship Foundation for their outstanding support during the study period.

I am also very grateful to Rotary Yoneyama Memorial Foundation for their support during my master course.

I am grateful to all my colleagues of Tokyo Institute of Technology during my master and Ph.D studies, especially to Prof. Koji Ito, Prof. Xin-Zhi Zheng and Prof. Katsunari Shibata.

I am grateful to all the colleagues of The Jikei University School of Medicine during my research on Master-Slave Robot for Endoscopic Surgery.

I am grateful to all the colleagues of The University of Electro-Communications during my undergraduate study, especially to Prof. Kazuo Yamafuji and Prof. Takayuki Tanaka.

I would like to thank all my colleagues of Niihama National College of Technology during my college study, especially to Prof. Yoshifumi Taniguchi, Prof. Koji Onishi and Prof. Tsuyoshi Miyata for providing advice and support in the NHK Robot Contest.

I am grateful to all whom help me during my studies and living in Japan.

I am very grateful to my mother, father, sister and brother who supported me during all this year.

I would like to dedicate this work to my parents and grandparents who immigrated to Brazil in the 1950's and worked for so many years to establish our family in a new land.

Contents

List of Tables

Chapter 1

INTRODUCTION

In our daily life, we unconsciously move our body to accomplish a large variety of motions. After the infant phase, usually a small amount of adaptation in each motion is needed to deal with environmental changes like carrying different weights, drinking using various shapes of bottle, walking on different floor types. Especially in sports the need to adapt rapidly to various kinds of situations is required. In all these cases the adaptation of the human motor sensory system is needed to deal with these small changes. But before we become able to adapt to these small changes, we need to learn new motion patterns like walking, running, reaching, catching. (Fig. 1-1)

In order to understand how humans learn and adapt to new situation, two different modalities of experiments were conducted. One of the experiments deals with the modeling of the human control characteristics during step response and continuous task. This study will be explained in details in Chapter 3. In Chapter 4 experiments about walking and running motion when using different shoe sole thickness were conducted in order to analyze the EMG signals around the heel contact. In both these experiments the research was focused on the learning and adaptation behaviour of the subjects related to the motion and EMG signals.

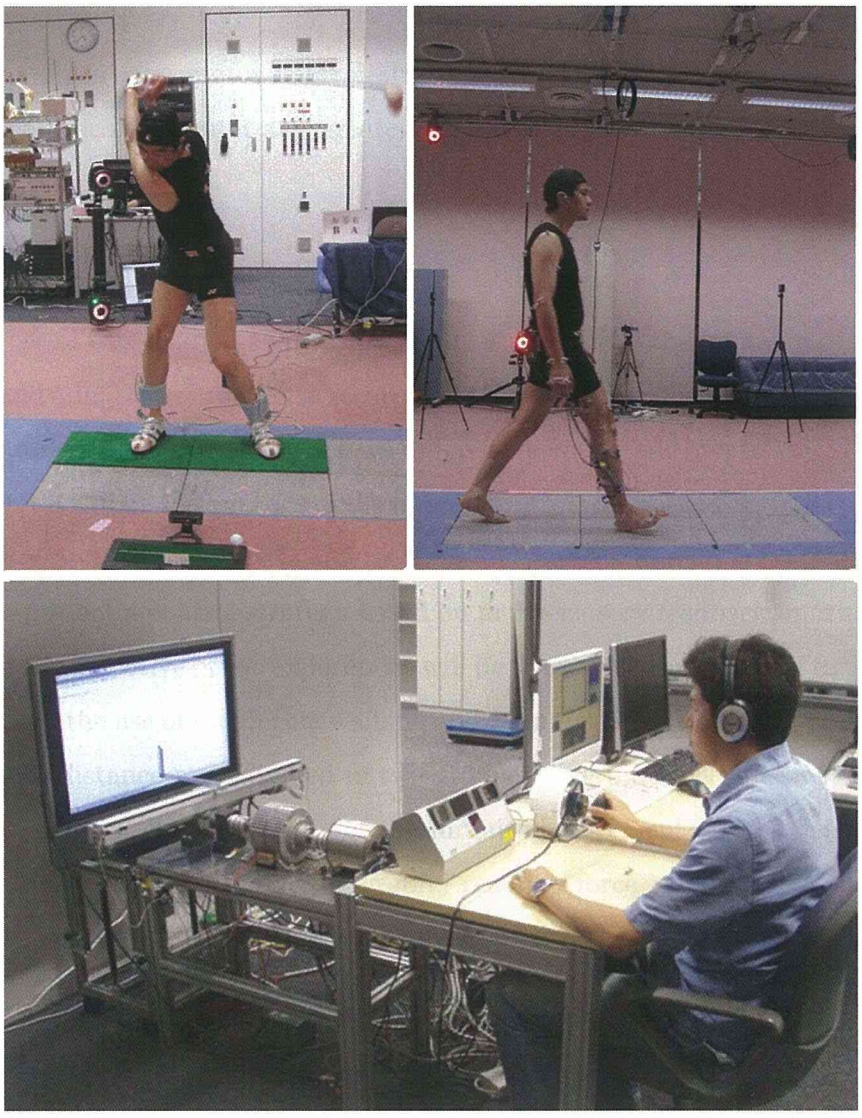

Figure 1-1: Example of daily life motions and experiment oriented tasks.

1.1 Motivations for human motor sensory learning and adaptation research

The author used to work on Master-Slave Endoscopic Surgery Robot, Bilateral Microteleoperation systems [27] [26] [25]. During this period the interest about how the human learn new motor control strategies and adapt to small changes in the environment become greater and greater.

1.2 Purpose

The purpose of this study is to measure, analyze and model the human motor sensory learning and adaptation process in terms of control theory and EMG signals. Here, the learning and adaptation terms will have different meaning and treatment. The aim of the Chapter 3 will be the analysis of the human control characteristics in respect to the visual, force and audio feedback information and build a human control model that can also represent a control strategy based on multi-sensory feedback information. In Chapter 4 the objective of the experiment will be to analyze the effects of different sole thickness and the use of toe during walking and running. A total of 15 athletes of short and medium distance were divided in two groups using different shoes with different sole thickness. Finally, the results of the initial measurement will be described and an evaluation method based on the ground reaction force and EMG signals will be proposed.

Chapter 2

MOTOR CONTROL LEARNING

2.1 Former Research

Since some decades ago, much research has been conducted focusing on how the human learn to move his/her own body despite the high degree of freedom and muscle activation redundancy [37]. During the early stages of infant age it is noted some flailing movements with the upper and lower limbs [34]. Also the motor speech coordination is not improved yet, which will have also an important role in social communication [38]. In most of the cases the motor learning is referred as the process to acquire a whole new motor coordination required for standing, walking and reaching motions, usually considering the infant. On the other hand, in some studies the reaching motion performed in an artificially generated environment is referred as learning and sometimes as adaptation. There are also many studies which proposed some models to explain the human motor control but after the learning stage. Hogan et al. [15] proposed a model to explain the quasi-straight hand trajectory model. Studies with frogs were elaborated [14] [28] to explain the scheme of internal model in terms of muscle activation and vector representation in the brain. In this chapter some insights about these both terms will be describe in order to clarify the usage of words learning and adaptation.

2.1.1 Feedback-error Learning

One of the most well known model to explain the motor learning scheme was proposed by Kawato et al.[19] [18] and it is based on feedback-error learning. In this model the summation of the feedback motor command and the feedforward command generated by the inverse model is fed to the controlled object. Then the feedback controller transforms the trajectory error into the motor-command error. The inverse model is trained using the difference between the desired trajectory and the actual trajectory. The more the inverse model approaches to the characteristic of the controlled object the error becomes smaller and the feedback controller input decreases. (Fig. 2-1)

2.1.2 Motor Control Adaptation

Shadmehr et al.[34] called motor adaptation as the recovery of performance within the changed mechanical environment. The adaptation level to the new environment was related to the aftereffects, which are the mirrored trajectories resulted from the adjustments made to compensate the force field. Furthermore, according to [4] "Adaptation refers to a process in which a system recovers previously learned skills after a change in the operating environment."

Investigations of Flash and Gurevich (1992) [7], Shadmehr and Mussa-Ivaldi (1994) [34], Sainburg and Ghez (1995) [33], and Gandolfo et al. (1996) [11] have demonstrated the presence of adaptive processes in the control of multijoint arm movements. In the conducted experiments, the subjects were required to execute point-to-point reaching movements while holding the handle of an instrumented manipulandum. In addition to these studies many researchers [32] [10] [9] [8] [16] [38] [34] [29] dealt with the issue of reaching tasks in the presence of force fields. Although, the majority called the after effects as a resulting of adaptation of the force field, they still used the term "learn" to move the arm during the training phase.

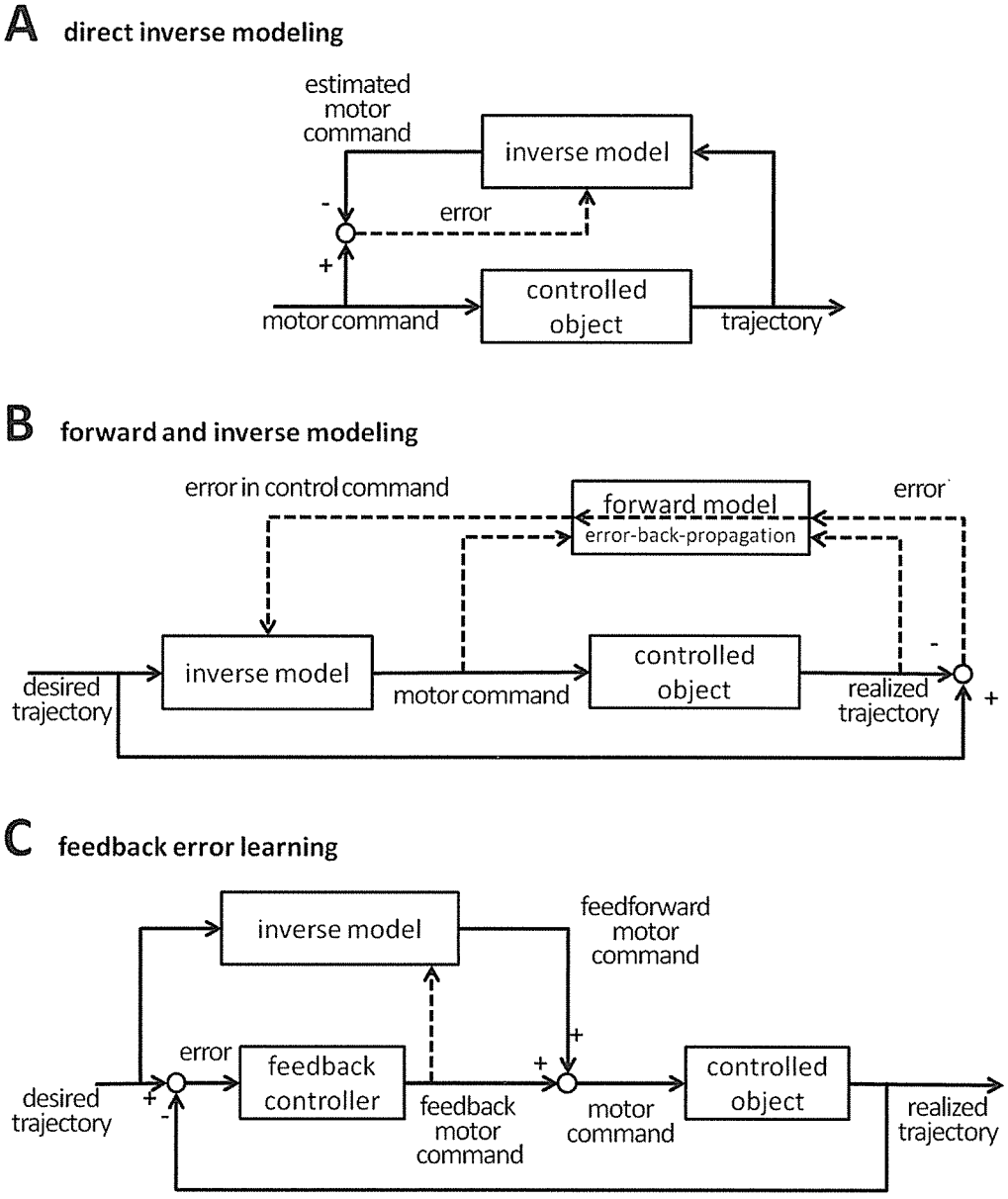

Figure 2-1: Three computational schemes for acquiring an inverse model through learning. Broken lines show information used for training. A Direct inverse modeling approach. B Forward and inverse modeling approach. C Feedback-error-learning approach. Modified from [19].

Chapter 3

HUMAN CONTROL MODEL BASED ON SENSORY FEEDBACK INFORMATION

3.1 Introduction

The human operator has the capability to learn, adapt and control various types of machines. It is of a great interest to understand how the human operator analyzes and processes different modalities of sensory feedback information in order to design directly or remotely operated machines. The aim of this study is to analyze the human control characteristics in respect to the visual, force and audio feedback information and build a human control model that can also represent a control strategy based on multi-sensory feedback (Fig.3-1). This model will be used to understand the learning and adaptation mechanism of human control strategy. In this primary work the time lag related to the human control model was measured using cognitive psychological experiments as single reaction time and choice reaction time. This control model would be useful to assist the design, simulation and evaluation of human-machine systems like telerobots [35] and also computer assisted systems as power-assist and drive-by-wire vehicles.

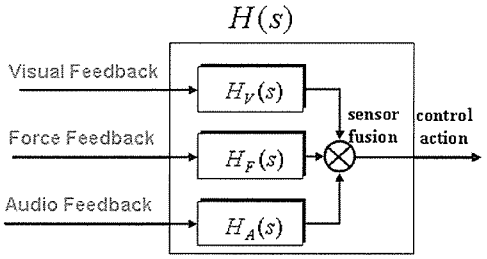

Figure 3-1: Multimodal sensory feedback scheme

3.2 Human Control Model

Early researches have already shown that it is important to consider the human dynamic characteristics when designing and evaluating man-machines systems. The major part of the analytical theory on manual control of vehicles was developed in the 60's. One of the important results was the Crossover Model proposed by McRuer et al. [24], which showed that the human-machine dynamic characteristics presented a first order lag near the crossover frequency (Fig.3-2). Another empirical result of McRuer [23] works showed that the human operator can change his dynamic characteristics according to the operated machine. A general model of the human control can be represented as Equation (3.3).

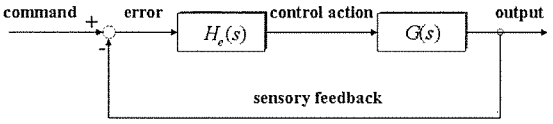

Figure 3-2: Generic human-machine system

$$H(s)G(s) \approx \frac{\omega_c e^{-\tau s}}{s} \qquad \text{(where, } \omega \approx \omega_c\text{)} \tag{3.1}$$

Here,

τ (0.1 - 0.4s) :Time lag due to human responses

ω_c(0.5 - 0.8Hz) :Crossover frequency

In this primary work the time lag due to human responses was measured using the single reaction time (SRT) and the choice reaction time (CRT).

3.3 Reaction Time Experiment

In order to identify the time lag due to human responses the single reaction time (SRT) and the choice reaction time (CRT) was measured with 3 subjects. The experiments were conducted using a master-slave type seesaw experimental device that was developed in order to analyze the human sensory feedback properties separately. It consists of a 1 DOF master haptic device with a force sensor that can be manipulated by rotating a dial or by gripping a joystick. The slave is an actuated linear guide that works as a seesaw with a sliding object over it. In the reaction time experiment 2 LEDs were used as visual cues, positioned at the left and right field of view of the subject (Fig.3-3). In most cases the reaction time is defined as the time necessary to the subject to turn the dial more than a pre-defined angle after the visual cue is presented. Since the final goal of the proposed human control model is to obtain an operator model of a continuous manipulation task, the reaction time was defined as the movement onset time. In this case, the movement onset corresponds to the time necessary to the dial's angular velocity reach 20 deg/s after the visual cue is presented. This velocity corresponds to about 1% of the maximum rotation velocity achieved by the subjects. During this experiment the gaze movement, pupil diameter and the pronator/supinator muscles EMG was also measured. The proposal for this study was reviewed by the Institutional Committee for Ergonomic Experiments and approved by the Director of Safety and Environmental Protection Department.

3.3.1 Single Reaction Time Experiment (SRT)

This experiment consists of moving the dial as fast as possible after the visual cue is shown to the subject. In SRT experiment the subject does not need to decide

Figure 3-3: Experimental device and reaction time experiment overview

which direction to move, it is a reflexive visuomotor action. After the subject became familiar with the experiment device 10 trials were made by each subject. The visual cue was presented randomly.

3.3.2 Choice Reaction Time Experiment (CRT)

In this experiment the subject has to decide in which direction to move according to the visual cue. If the right LED turns on the subject has to turn the dial in the clockwise direction. If the left LED turns on the subject has to rotate the dial in the counter clockwise direction. In this CRT experiment a computational load is added to the subject due to the decision making about which direction to move. The visual cue was shown randomly in time and direction. Here the reaction time was also defined as the movement onset time. After some training each subject performed 20 trials.

3.3.3 SRT and CRT Movement Onset Time Results

The movement onset time results of SRT and CRT experiments are shown in Table 3.1 and Table 3.2. The difference between the fastest subject C (0.20s) and slowest subject B (0.26s) subject was about 30% in SRT and more than 33% in CRT experiments. It is interesting to notice that even though the SRT onset time of subjects A and

C are very close, the CRT onset time varied considerable. Further considerations will be discussed together with the measurement results. Fig.3-4 and Fig.3-5 showed typical angle and velocity profiles respectively. In both profiles a similarity can be noticed between the subjects A and C. All the subjects showed a pre-programmed target angle which is reached about 0.6s-0.8s after the movement onset. (Fig.3-4).

Table 3.1: SRT Experiment - EMG Activation and Onset Time

Experiment	Subject A	Subject B	Subject C
Onset [s]	0.21 ± 0.03	0.26 ± 0.04	0.20 ± 0.03
EMG-RT[s]	0.19 ± 0.04	0.21 ± 0.04	0.15 ± 0.03
EMD [s]	0.03 ± 0.02	0.05 ± 0.01	0.05 ± 0.01

Table 3.2: CRT Experiment - EMG Activation and Onset Time

Experiment	Subject A	Subject B	Subject C
Onset [s]	0.24 ± 0.02	0.32 ± 0.05	0.27 ± 0.04
EMG-RT[s]	0.19 ± 0.02	0.28 ± 0.04	0.20 ± 0.04
EMD [s]	0.04 ± 0.01	0.04 ± 0.02	0.06 ± 0.03

SRT and CRT EMG Measurement Results

From Fig.3-6, Fig.3-7, Fig.3-8 and Fig.3-9 it can be noticed that the activation of pronator and supinator muscles occurred before the actual movement started. The time necessary to send the motor command after the visual information was acquired varied from 0.15s to 0.19s in SRT experiments and 0.19s to 0.28s in CRT experiments. This time includes the decision making time and motor command activation which are difficult to identify separately.Thus it can be inferred that the time to make a decision varied from nearly 0s in Subject A to 0.07s in Subject B.

Due to the musculoskeletal and the haptic inertial properties another approximately 0.05s were necessary until the movement actually started. The time between

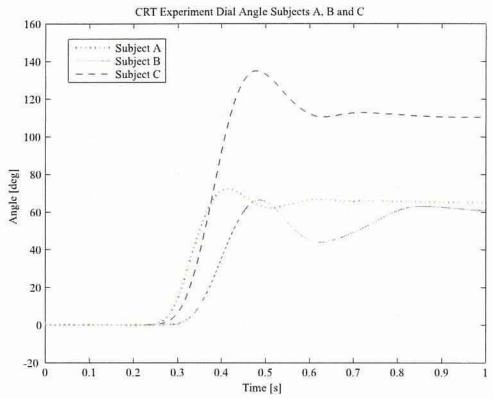

Figure 3-4: CRT experiment.Angle profile os subjects A, B, C

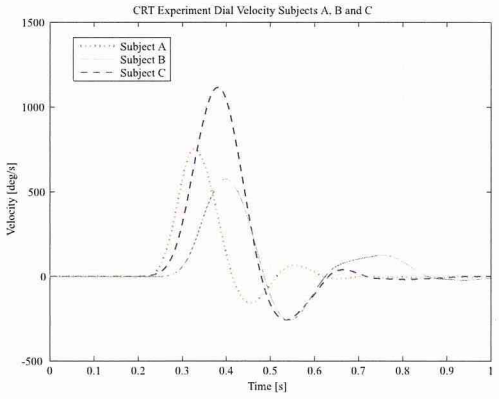

Figure 3-5: CRT experiment. Velocity profile of subjects A, B, C

the visual cue and the emergence of EMG is called ElectroMyoGraphical Reaction Time: EMG-RT or PreMotor Time. ElectroMechanical Delay: EMD is defined as the time between the EMG activation and the starting of the movement. In this case the movement onset. It corresponds to the elctromechanical characteristics of the muscles [20].

From the results of EMG-RT of SRT and CRT experiments it can be noticed that subject A showed a very fast decision making response since there were no significant difference between the two experiments. On the other hand, the EMD time was relatively longer compared to subjects B and C. This short latency can be inferred as a resultant of a more effective preactivation of motor patterns since the movement is already known. See Fig.3-6 and Fig.3-7. In the case of subjects B and C, the EMD time of SRT and CRT experiments were almost the same. Thus, there is a possibility that the subjects were not in a "fight or flight" state. Even though the SRT onset time of subjects A and C were similar, the considerable difference in CRT experiments is presumed to be attributed to the proficiency of the decision making loop. It can be noticed from a typical trial in Fig.3-7 that the motor activation of subject A is faster than subject C showed in Fig.3-9.

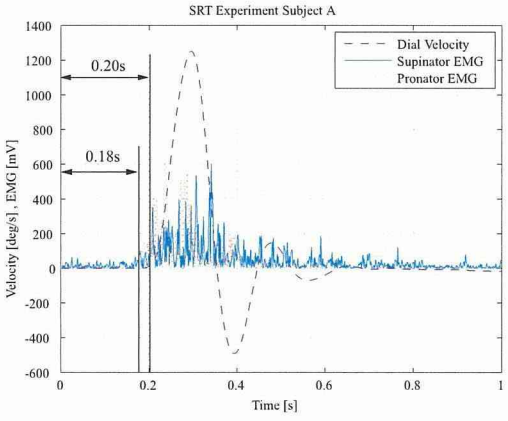

Figure 3-6: SRT experiment - Subject A

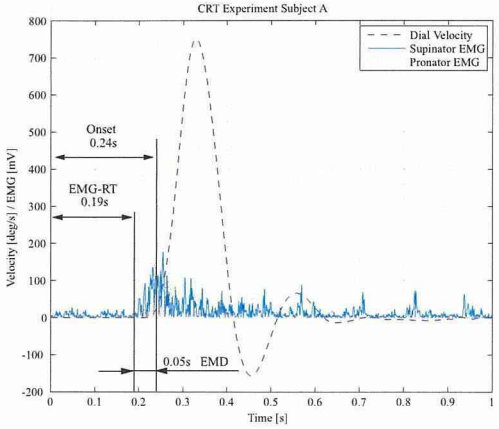

Figure 3-7: CRT experiment - Subject A

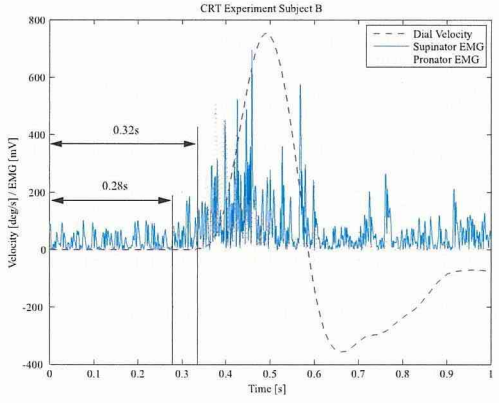

Figure 3-8: CRT experiment - Subject B

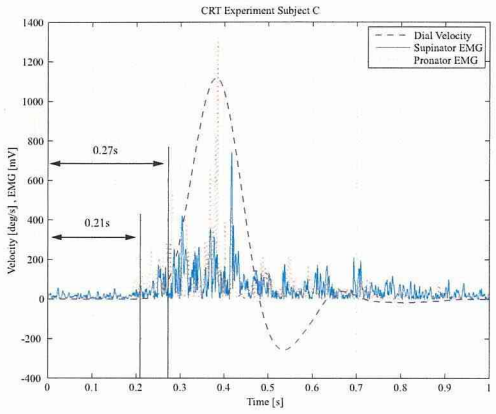

Figure 3-9: CRT Experiment - Subject C

SRT and CRT Gaze Movement and Pupil Diameter

The significant difference between the decision time in subject A and B can probably be related to the gaze movement, i.e. the strategy chosen by the subject to acquire visual information. The fastest subject A used mainly the peripheral vision to cognize which LED turned on because he had his eyes fixed in the middle of the right and left LEDs (Fig.3-10). On the other hand the slowest subject B used his central vision to identify which visual cue was presented moving his eyes from left to right and vice-versa (Fig.3-11). Subject C also performed a similar strategy to subject A (Fig.3-12). The thick vertical line indicates when the visual cue was presented to the subject. The reaction time related to these different types of strategy became even more accentuated when the gaze movement coincided with the visual cue presentation like in trial of Fig.3-11. This contributed to a slow response action by the subject B. The pupil diameter was also measured in these experiments (green dashed line in Fig.3-10, Fig.3-11, Fig.3-12). The discontinuity is due to eye blinking. A slightly retraction of pupil can be noticed when the visual cue is presented but it depended on the trial, not being as prominent as expected.

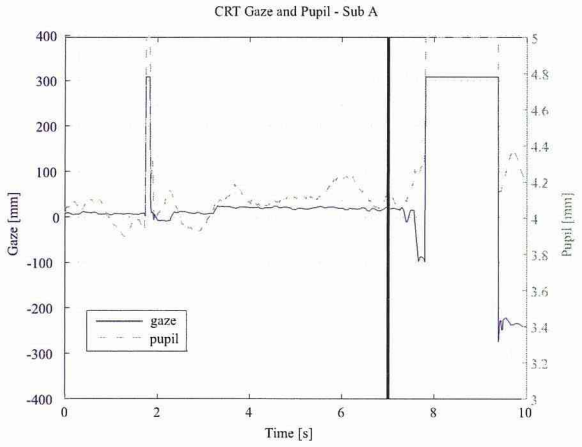

Figure 3-10: CRT experiment subject A (cue at 7.0s). The solid line represents gaze movement and the dashed line pupil diameter variation. Use of peripheral vision. The discontinuity is due to eye blinking.

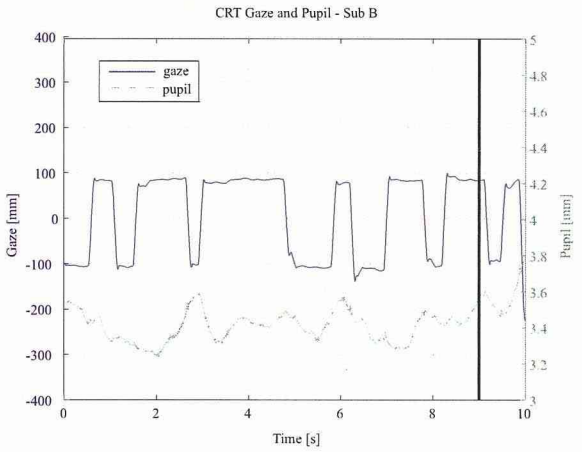

Figure 3-11: CRT experiment subject B. The solid line represents gaze movement and the dashed line pupil diameter variation. Use of central vision.

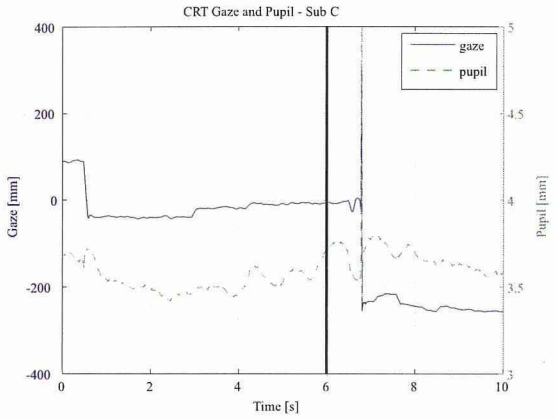

Figure 3-12: CRT experiment subject C. Gaze and pupil diameter.

3.3.4 Step Response Parameter Estimation

In order to model the human control characteristics, it is necessary to identify the control parameters using system identification method. Here, a step response identification using the reaction time experiment data was conducted to estimate the human response time which corresponds to the time delay.

From Fig. 3-4 it can be noticed that the angle profiles of the subjects are similar to a step response (Fig. 3-13). Based on Eq.3.2 the step response parameters were identified using Matlab Identification Toolbox. The time delay estimated from step response was compared to that one measured directly in the reaction time experiment. It can be noticed that the estimated time delay were bigger than the measured movement onset time. See Table 3.1, Table 3.2 and Table 3.3, Table 3.4. This difference can be attributed to the limitation of the step response identification to express the initial rising phase. Although there is a slightly discrepancy in the numerical value of the time delay, the estimated function represents well the measured data (Fig. 3-14).

$$H(s) = \frac{K{\omega_n}^2}{s^2 + 2\zeta\omega_n s + {\omega_n}^2} e^{-\tau_d s} \tag{3.2}$$

Here,

K :Gain, proportional to final value

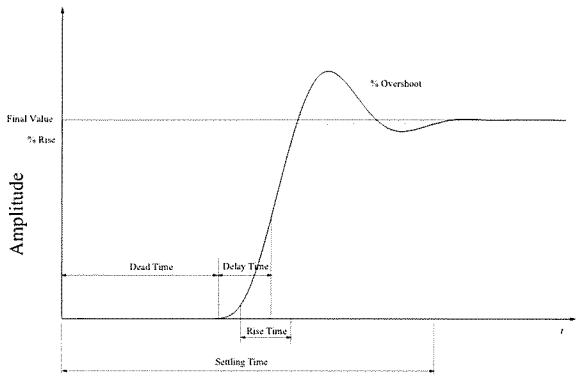

Figure 3-13: 4 Step Response Parameter Estimation

τ_d :Time lag due to human responses

ω_n :Natural angular frequency

ζ :Damping ratio

Table 3.3: Estimation of time lag from step response - SRT

Parameters	Subject A	Subject B	Subject C
ω_n [rad/s]	27 ± 2	15 ± 5	20 ± 2
ζ	0.34 ± 0.04	0.48 ± 0.08	0.50 ± 0.03
τ_d [s]	0.24 ± 0.03	0.29 ± 0.04	0.26 ± 0.03

Table 3.4: Estimation of time lag from step response - CRT

Parameters	Subject A	Subject B	Subject C
ω_n [rad/s]	27 ± 2	18 ± 6	18 ± 2
ζ	0.46 ± 0.11	0.40 ± 0.01	0.52 ± 0.06
τ_d [s]	0.28 ± 0.03	0.36 ± 0.05	0.31 ± 0.04

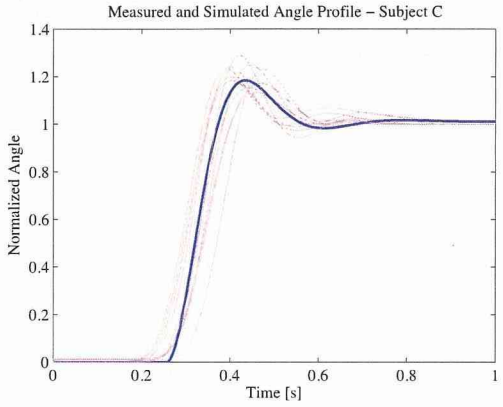

Figure 3-14: SRT experiment measured and simulated angle profile. The thin lines represents the measured 10 trials and the thick line the estimated output. Subject C.

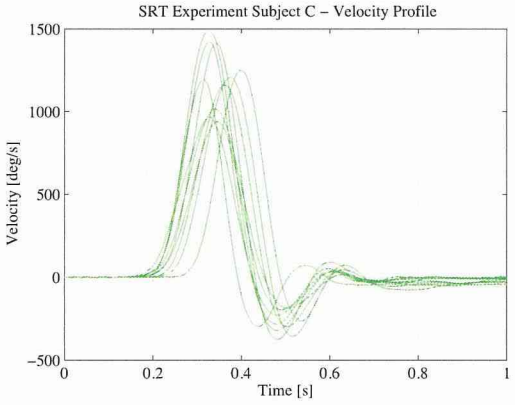

Figure 3-15: SRT experiment velocity profile. Subject C.

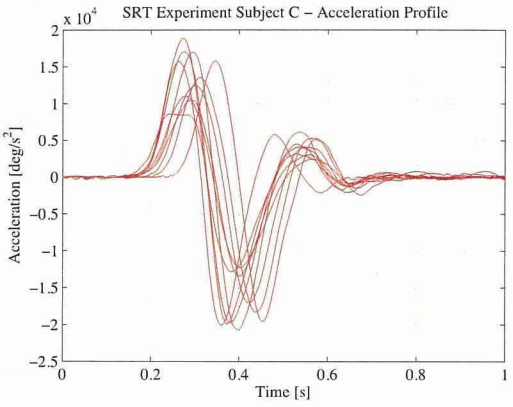

Figure 3-16: SRT experiment acceleration profile. Subject C.

3.3.5 Discussion

First, the movement onset, EMG-RT and the EMD delay will be discussed. An interesting fact was found during subject A reaction time measurement. A more significant difference was expected between SRT and CRT EMG-RT, but there were almost the same. On the other hand, the EMD delay differed and the onset time increased as expected. From these facts some speculations about the formation of a preplanned movement strategy can be inferred to explain different EMD delays. But further EMG measurements should be conducted to clarify this hypothesis. An increase of pupil diameter was also expected due to the concentration in the task, but no significant changes were found nor there were a correlation between the pupil diamater and the gaze movement.

Second, it was shown that there is a numerical discrepancy between the reaction time obtained directly from measurement experiment and the time delay estimated from step response identification. Nevertheless this should be treated as crucial deficiency of a human control characteristics system identification. Actually, the estimated time delay represents well the human response, since there were a small and constant difference of 0.4s-0.6s between each subject's onset time and the time delay. In order to obtain a more precisely value about the reaction time, a directly measurement is recommended, including also an EMG measurement. Otherwise the error

of the estimated time delay should be considered during the system identification of human control properties.

In the next section analysis about the relation between the EMG activation and the identified parameters such as time delay, natural angular frequency and the damping ratio will be conducted and also a comparative study with the psychophysiological measurements of the human operator will be discussed.

3.3.6 Conclusions

This first part of the human control model research measured the reaction time and the step respose characteristic represented as a transfer function. In order to identify each control parameter, first the time lag was measured since SRT and CRT are directly associated with the human responses. This work measured the human time responses related to visual perception, motor command and decision making. The onset time, EMG-RT and the EMD delay was measured and compared to the time lag estimated from step response identification. Although a small discrepancy was found between the directly measured time lag and the estimated one, the system identification method showed a prominent and methodological approach to model the human control system.

3.4 HUMAN CONTROL MODEL IN CONTINOUS TASK

In the previous section the results about reaction time measurement and the human model related to step response experiment were shown. Although, in order to simulate the human control behaviour during a manipulation task it is necessary to measure and analyze the human control characteristics in a continuous task. In this section the measurement of the reaction time will be compared to the time delay identified during a visual tracking task using only visual feedback and with force feedback information. An experiment device capable of measuring the human control characteristics in the

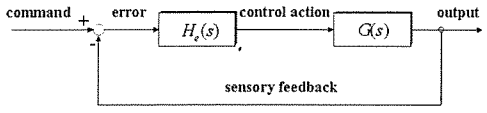

Figure 3-17: Human Machine Block System

presence of different sensory feedback information was developed.

3.4.1 Visual Feedback

One result of McRuer [24] [23] works about the analytical theory on manual control of vehicles was the Crossover Model. See Eq. 3.3 and Fig. 3-17. According to the manipulated machine characteristics the human operator can modify his/her own dynamic characteristics so as the open-loop transfer function remains a first order system.

$G(s)$ represents the machine dynamics.

$$H(s)G(s) \approx \frac{\omega_c e^{-\tau s}}{s} \qquad (near\ \omega_c) \tag{3.3}$$

where, τ (0.1 $\sim$ 0.4s) represents the time lag due to human responses, ω_c (0.5 $\sim$ 0.8Hz) is the crossover frequency.

3.4.2 Force Feedback

The force feedback felt by the human operator is a result of a combination of tactile sensors and proprioceptive feedback. Although the individuals properties of each sensor have been studied, how the human operator uses those information and how they affect the human control characteristics are still not well known. However, it is of general agreement that the force feedback information is very important to identify the controlled object dynamics properties.

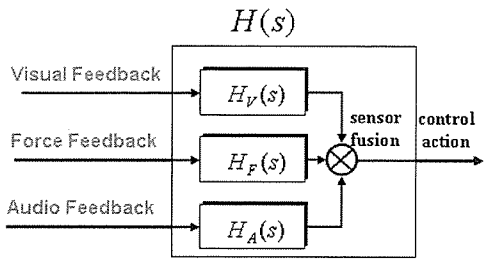

Figure 3-18: Multimodal sensory feedback scheme

3.4.3 Audio Feedback

A primary function of audio feedback is said to direct the eyes to the source of the sound. More specifically in a tracking task the audio feedback provides information about the localization and velocity of the moving target. Although the space discrimination of auditory localization is not so accurate (about 15 degrees) compared to the visual, it provides supplementary information to assist other sensory feedback.

3.4.4 Human Control Model based on Multimodal Sensory Feedback

This work proposes a human control model based on multiple sensory feedback information. (See Fig. 3-18). The human control characteristics related to visual, force and audio feedback information will be measured separately and then a combination of different sensory feedback will be analyzed in order to understand how the human operator uses these sensory feedback information to acquire an internal model of the controlled machine. First, in this work, the analysis of the human control strategy in the presence of visual, force and the combination of visual and force feedback information was conducted.

3.4.5 Experiments

Two types of experiments were conducted. First, the human reaction time was measured. The second experiment is based on visual tracking in the absence and pres-

Figure 3-19: SEesaw Experimental Device (SEED)

ence of force feedback. The proposal for this study was reviewed by the Institutional Committee for Ergonomic Experiments and approved by the Director of Safety and Environmental Protection Department.

3.4.6 Operator Control Characteristics Identification Experiment

The method to model the human operator adopted in this study is based basically in the system identification used in control theory. However, it is crucial to select a task that can provide an analysis of the operator characteristics in a visual and force control manipulation independently, i.e. a task that can be performed with only one type of sensory feedback information. It is also preferable to be a continuous task for system identification analysis in a wide frequency range. The peg-in-hole task is widely used as an example of robot control, but it is very hard to decompose the position and force control strategies. The inverted pendulum is also commonly used to demonstrate different control methods. However, it is a task very difficult to accomplish with the eyes closed. After considering many tasks performed by a human operator, the control of a slider on a seesaw was chosen as a suitable task that can

pull together all the necessary features to analyze and identify the human-machine system related to visual, force and also audio feedback information independently. To analyze the human control characteristics related to different sensory feedback properties a master-slave type SEesaw Experimental Device (SEED) was developed. The master haptic device consists of a dial with a force sensor and the slave is an actuated linear guide that works as a seesaw bar with a slider over it. (See Fig. 3-19 and Fig. 3-20). After analyzing the control characteristics based on visual ($H_v(s)$), force ($H_f(s)$) sensory feedback information separately, the combination visual and force feedback ($H_{vf}(s)$) was analyzed.

3.4.7 Visual Pursuit Tracking with a Normal Slider

In this first experiment to analyze the human visual feedback properties, the human operator manipulates the master dial in order to make the slider, PD controlled, follow a random reference signal displayed in a monitor. The machine characteristics is a first order system. After 20 training trials, 10 trials were measured. Fig. 3-21 shows the reference signal, the measured data and the output of the identified operator model. The technique used to identify the human operator's characteristics is common to all the following two experiments. First, it was assumed that the human-machine open loop transfer function has the generalized form of Eq. (3.4).

$$H(s) = K\frac{(1+T_L s)}{(1+T_I s)}e^{-\tau s} \tag{3.4}$$

where K represents proportional gain, $e^{-\tau s}$: time delay due to human response, $(1+T_L s)$ is the lead time constant (relative rate-to-displacement), $(1+T_I s)^{-1}$ is the lag time constant.

Using the process model identification of Matlab toolbox the appropriate parameters were calculated by minimizing the error between the model output and the measured data. By this search the most suitable form was selected and then the time delay which corresponds to the smaller fitting error was explored. In all the cases a priori knowledge about the controlled machine was used in order to obtain the oper-

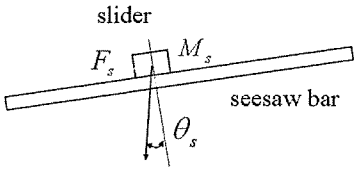

Figure 3-20: Seesaw and slider model

ator characteristics. After obtaining the parameters, they were averaged separately and the results are shown in Table 3.5.

3.4.8 Visual Feedback using a Seesaw Task

Here the subject is instructed to follow the random reference signal as the previous experiment. But this time the machine dynamics behaves as a slider over a seesaw, i.e. like Eq. (3.5). There is no force feedback. After some practice the subject is able to execute successfully the task. To avoid the subject to notice that the slider behavior corresponds to a seesaw task, the seesaw bar was maintained in horizontal position.

$$(\theta_s \approx 0 \Rightarrow sin\theta_s \approx \theta_s) \qquad G(s) = \frac{x_s}{\theta_s} = \frac{g}{s^2} \tag{3.5}$$

where g is the gravity, θ_s is the seesaw bar inclination, x_s is the slider position and s is the Laplace operator

3.4.9 Visual and Force Feedback using a Seesaw Task

In this task the subject has to follow a random reference signal feeling the torque caused by the dislocation of the slider over the seesaw. The proficiency in the task execution was similar to the visual feedback solely, but the human modeling error increased due to the need of extra operational force. (Fig. 3-26).

Table 3.5: Identified Human Control Model

Experiment	Subject A	Subject B	Subject C
Pursuit $H_p(s)$	$\frac{2.3}{1+0.4s}e^{-0.20s}$	$\frac{2.1}{1+0.6s}e^{-0.27s}$	$\frac{2.2}{1+0.5s}e^{-0.22s}$
Visual $H_v(s)$	$6\frac{1+4s}{1+0.06s}e^{-0.24s}$	$4\frac{1+4s}{1+0.2s}e^{-0.31s}$	$10\frac{1+2s}{1+0.03s}e^{-0.21s}$
Visual/Force $H_{vf}(s)$	$10\frac{1+2s}{1+0.04s}e^{-0.23s}$	$8\frac{1+2s}{1+0.1s}e^{-0.29s}$	$13\frac{1+2s}{1+0.04s}e^{-0.22s}$

3.4.10 Force Feedback using a Seesaw Task

In this task the subject has to maintain the slider at the centre using only the force feedback information provided by the haptic dial. The slider is pertubated by a random force with a cuttoff frequency of 0.2 Hz. This task is very difficult to accomplish and requires much more trainning than the previous tasks.

3.4.11 Human Control Characteristics Experiment Results

The results of identified human control characteristics are shown in Table 3.5. The human control model related to visual pursuit task showed a first order characteristic. Comparing the three subjects it can be noticed that the lag time element T_I is proportional to the correspondent time delay τ . Fig. 3-21 shows the reference target, the measured data and the control model output of the identified mean human model. The model output has the same behavior of the human operator except the high frequency features.

In the case of seesaw task using visual feedback with or without the presence of force feedback, all the subjects presented a lead time element T_L. This lead time element is responsible for the prediction of the slider's behavior. Due to the high acceleration of the gravity, a predictive element was necessary to make possible the control by the human operator.

The presence of force feedback had the effect of decreasing the time constant and increasing the gain element. The latter one can be attributed to the high stiffness of the forearm because of the haptic feedback.

Human control model of Sub A in visual pursuit task.

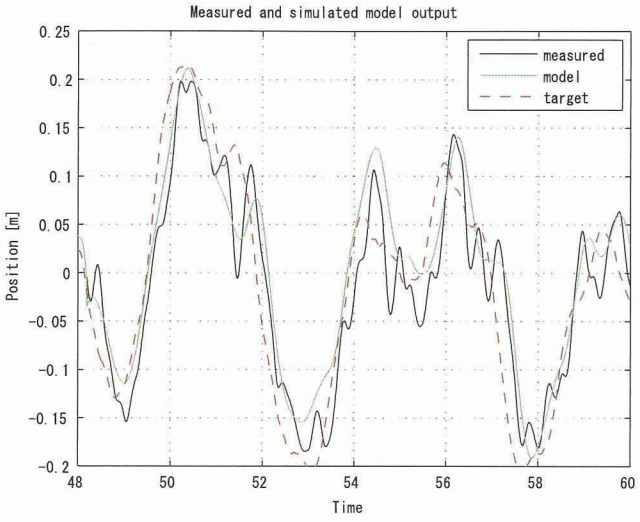

Figure 3-21: Visual pursuit experiment.

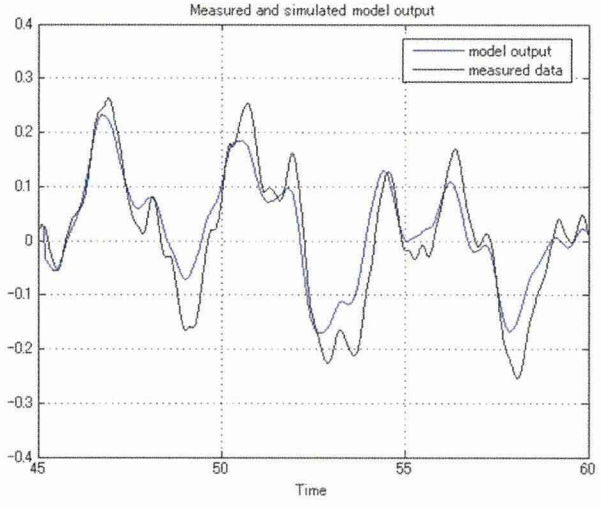

Figure 3-22: Visual pursuit experiment (Sub A).

$$H^A(s) = 2.3\frac{1}{(1+0.4)}e^{-0.20s} \tag{3.6}$$

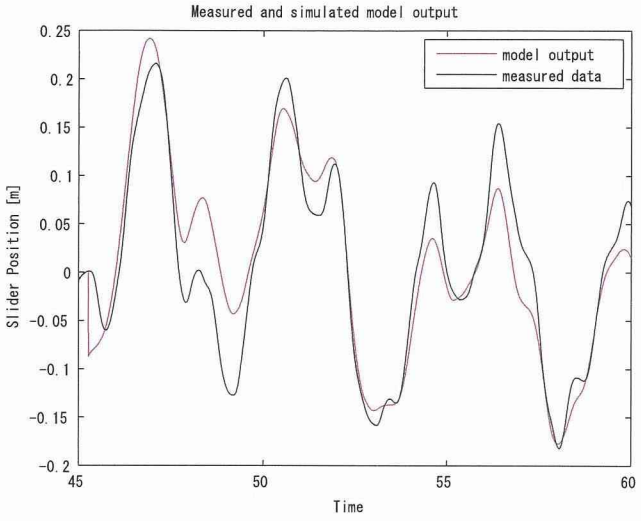

Figure 3-23: Visual pursuit experiment (Sub B).

Human control model of Sub B in visual pursuit task.

$$H^B(s) = 2.1\frac{1}{(1+0.6)}e^{-0.27s} \tag{3.7}$$

Human control model of Sub A in visual feedback seesaw task.

$$H_V^A(s) = -2\frac{20s+1}{(16s+1)}e^{-0.5s} \tag{3.8}$$

Human control model of Sub A in visual and force feedback seesaw task.

$$H_{VF}^A(s) = 10\frac{1+2s}{(1+0.04)}e^{-0.23s} \tag{3.9}$$

Human control model of Sub D in force feedback seesaw task.

$$H_F^D(s) = 6\frac{1+4s}{(1+0.06)}e^{-0.24s} \tag{3.10}$$

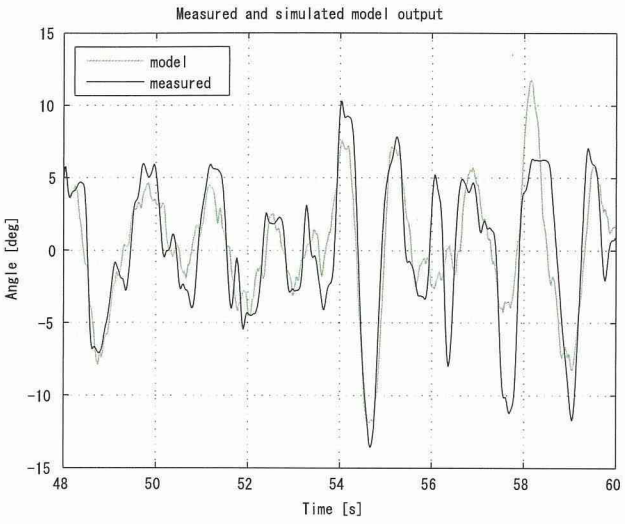

Figure 3-24: Seesaw task experiment using only visual feedback information.

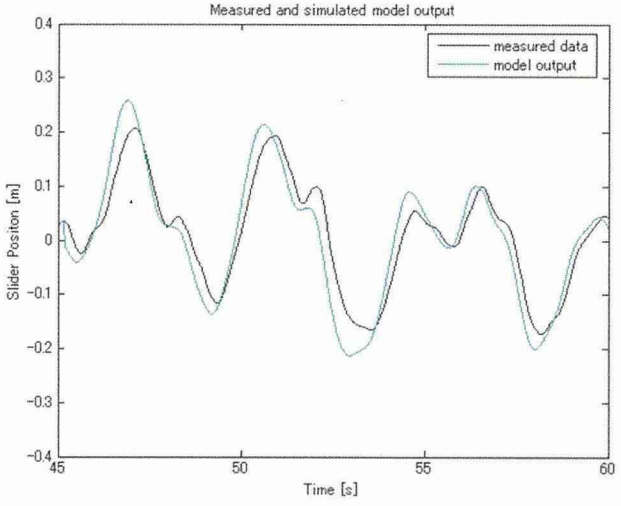

Figure 3-25: Seesaw task experiment using visual feedback information. (Sub A).

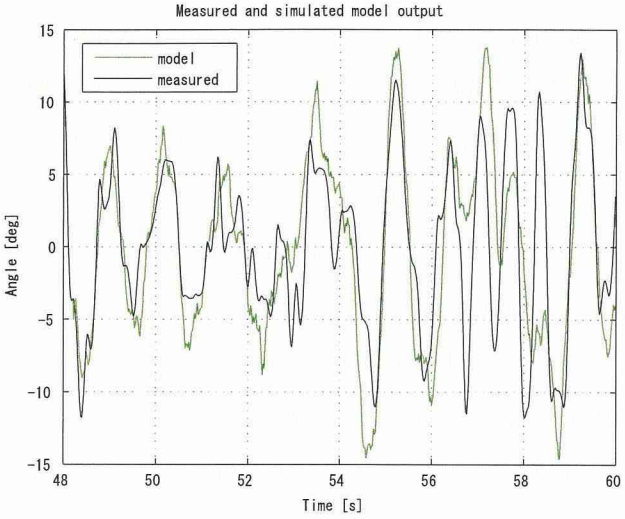

Figure 3-26: Seesaw task experiment using visual and force feedback information.

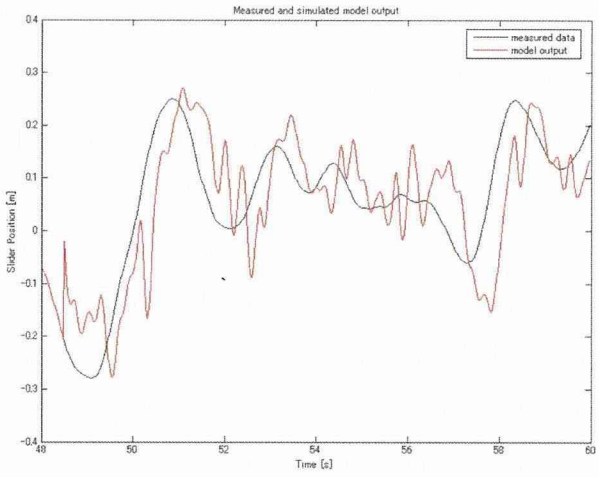

Figure 3-27: Seesaw task experiment using only force feedback information. (Sub D).

3.4.12 Discussion

From Table 3.5, it can be noticed that according to the characteristics of the task the time delay identified has different values. But the relation between subjects is preserved as the subject B has the biggest time delay. Although the time delay is different from the RT experiment results, the direct measurement of the human response time presents a reasonable and practical method of identifying the time delay reducing the number of parameters to be fitted. Further investigation about the muscle activation time and neuromuscular dynamics should be conducted to achieve a better estimation of the human response delay. The human control model represented here as a transfer function was identified after each subject had performed many training trials, because the parameter estimation had to be executed in a stable condition. In this way, the estimated transfer function expresses the learned human control model. Furthermore, the difference in the order of the transfer functions when manipulating various machine characteristics represented the learned control model. On the other side small variation in the parameters due to the presence of different sensory information can be correlated to the subject's capability of adaptation.

3.4.13 Conclusion

The direct measurement of the reaction time using also EMG signals gave insights about the individual variation between subjects showing that the EMG-RT time was responsible for such difference. This measured reaction time was also correlated to the time delay estimated from continuous pursuit tracking task. It was shown that the human acquired model depended on the machine characteristics and the learned model was associated with the transfer function order. When different sensorial information was available to the subjects, there were noted small variations in the transfer function parameters representing the subjects capability to adapt to different sensorial feedback information.

This section proposed an analytical method using the SEED to identify the human control characteristics related different sensory feedback information. The hu-

man model related to visual feedback solely and visual/force feedback was identified using the techniques of identification methods. It is important to notice that all the experiments were performed without audio information. There still work to be done in order to build a human sensory feedback integration model to represent the human operator including also the audio feedback information. These sensorial feedback information are believed to play an important role in the acquisition of the internal model of manipulated machines.

Chapter 4

EFFECTS OF TOE MOVEMENT DURING WALKING AND RUNNING IN TERMS OF GRF AND EMG SIGNALS

In order to analyze the motor learning and adaptation of a daily activity movement the walking/running task was selected. However, to provide the subject a different environment different shoes were chosen for these experiments. The objective of this experiment is to analyze the effects of different sole thickness and the use of toe during walking and running in terms of learning and adaptation of the motor control strategy. A total of 15 athletes of short and medium distance were divided in two groups using different shoes. From GRF and EMG results it can be inferred that the toe movement inside a thick sole shoe does not affect the forces patterns between the foot and the ground, making this kind of movement meaningless in terms of shock absorption. The toe movement caused an ankle joint torque to increase about 20% in the midstance phase compared to the normal barefoot gait. The results about the effects of toe movement in barefoot and shod walking/running will be used to establish an evaluation method to assess the performance of the two groups.

KEY WORDS Gait Analysis, Ground Reaction Force, Ankle Joint Torque Estimation, EMG signals, Shock Absorption

4.1 Introduction

In the ancient times before the development of footwear, the human gait required all the foot and leg active and passive properties in order to walk on very different ground surfaces. Especially the Plantaris muscle is believed to have an important role in shock absorption because it can contribute to the formation of foot arch by flexing the metatarsophalangeal joints (MTP) [5]. On the other hand the every day use of thick sole and closed-toe shoe is pointed as one cause of flat foot among children [31]. In order to avoid such problems and improve the natural human capability of active shock absorption, measurements about gait and running motions wearing various types of footwear was initiated. This is the first report of a 6 months long term experiment which consists in 3 phases: before, during, after the use of specific type of footwear. The objective of this long term experiment is to analyze the effects of different sole thickness and the use of toe during walking and running. A total of 15 athletes of short and medium distance were divided in two groups using different shoes with different sole thickness. Here the first results of the initial measurement are described and an evaluation method based on the ground reaction force and EMG signals is proposed.

4.2 Methods

4.2.1 Experiment Overview

First 5 male subjects (age average 19.2 ± 1.0 years) participated in this primary stage. Every subject had to perform 3 trials of walking and running motions in barefoot and shod conditions. The walking velocity was defined as 5km/h and the running velocity was 10km/h. The tolerance of velocity variation was 5% and it was measured in real time and feedback to the subjects.

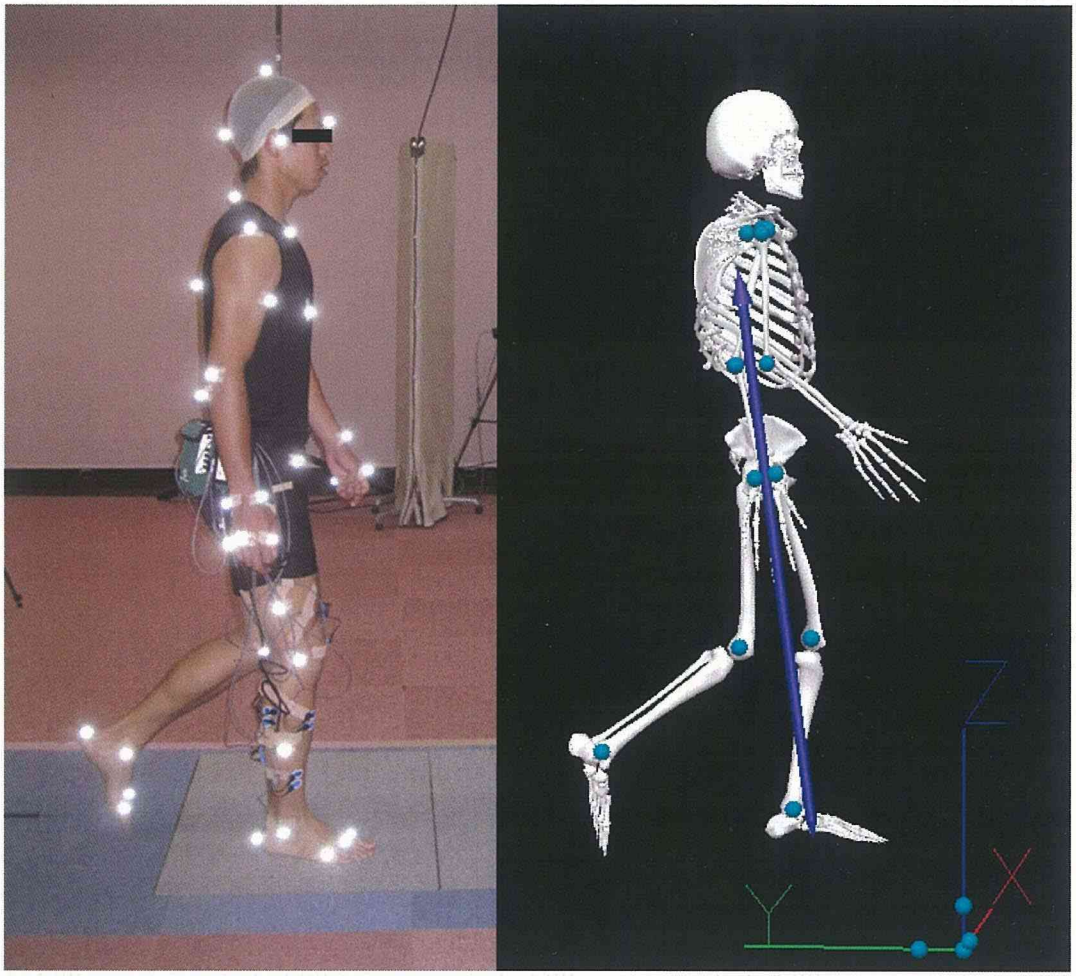

Figure 4-1: Experiment overview and the kinematic/kinetic model built using Visual 3D

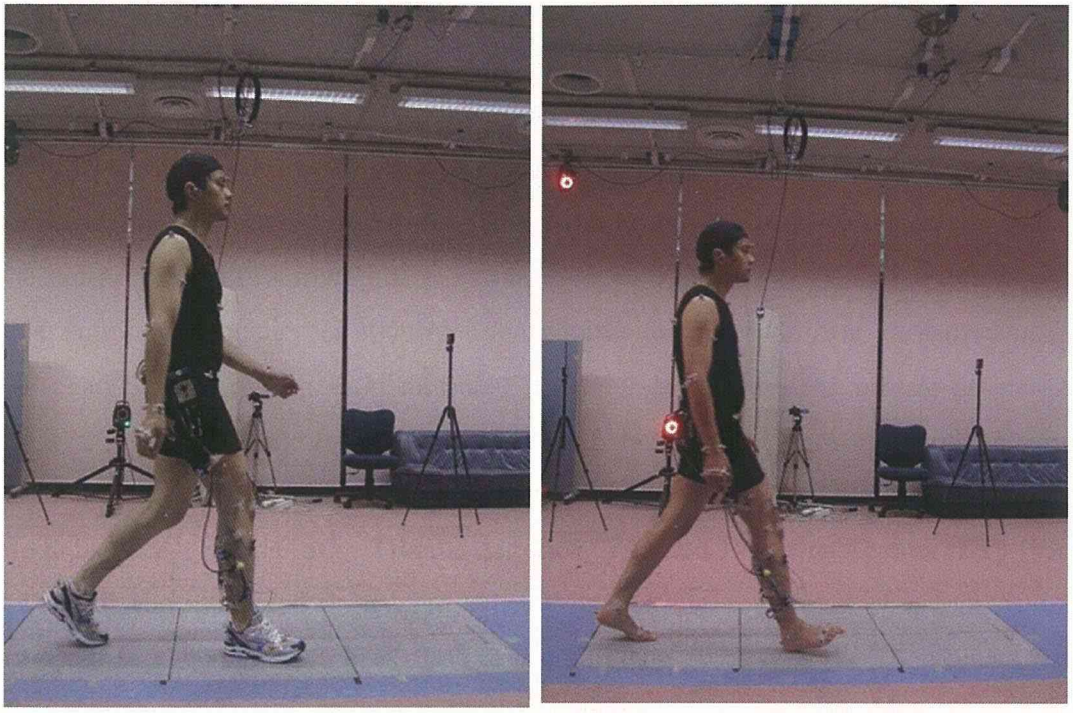

Figure 4-2: Barefoot and Shod Walking Task

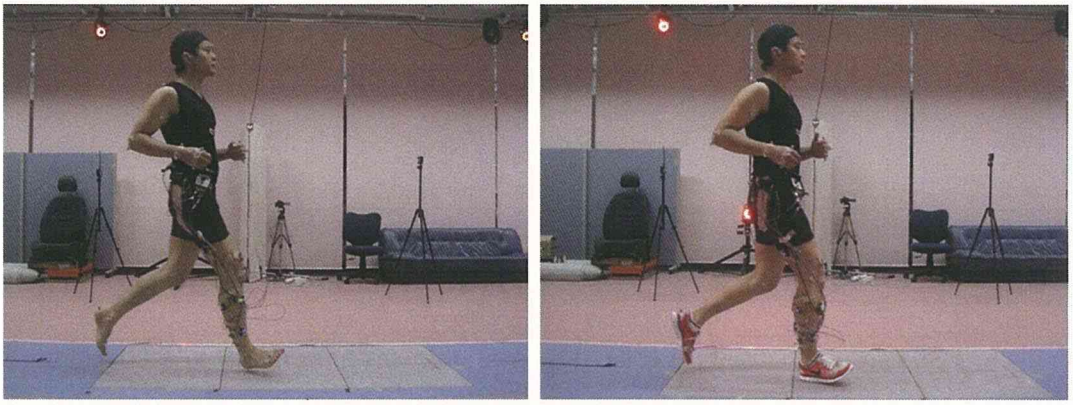

Figure 4-3: Barefoot and Shod Running Task

4.2.2 Measurement

The gait and running motion were measured using a 3D motion capture Vicon system with 10 cameras at a sampling frequency of 250Hz. A total of 53 reflective markers were attached to the subject. The experimental overview, the motion captured model and the model made by Visual 3D and used for kinematic and kinetic analysis are shown in Fig. 4-1.In the case of shod walking/running the markers were attached to the shoes. Six AMTI Force Platforms were used to measure the ground reaction force at a sampling frequency of 1000Hz. The plantar foot pressure was measured using a F-Scan System during shod motions. In order to analyze the muscle activation the surface EMG of the following 7 muscles of the right leg were measured: Vastus Medialis (VM), Biceps Femoris (BF), Gastrocnemius Lateralis (GL), Gastrocnemius Medialis (GM), Soleus (SO), Tibialis Anterior (TA) and Peroneus Tertius (PT) (Fig. 4-5). All the measured data were synchronized using the signal of a foot switch attached to the right foot heel. Before dividing the groups all the 15 subjects had their foot shape measured to check the arch height and avoid bias in the results (Fig. 4-7). All the subjects were confirmed as heel strike runners. The shoes used for shod walking and running were a typical jogging shoe with relative thick sole (about 30mm at the heel) and another with thin sole (about 20mm at the heel). Besides the normal walking and running the subject was instructed to move his toe as he intended to grab the ground with his toes. This motion using the toes is called here Toe Walk and Toe Run respectively.

4.3 Results

4.3.1 Ground Reaction Force

From the data of the ground reaction force (GRF) it is clear to see the effect of shock absorption during the heel contact (HC) represented by the first peak in the graphs of Fig. 4-8, Fig. 4-9, Fig. 4-10, Fig. 4-11, Fig. 4-12, Fig. 4-13. In the case of barefoot running, the first peak is very sharp but in the midstance phase there is a

Figure 4-4: Types of shoes used in the experiment

slight difference caused probably by the toe movement which increased the plantar stiffness and created a foot arch (Fig. 4-8 and Fig. 4-9). A similar phenomenon can be observed when the sole is thin (Fig. 4-10 and Fig. 4-11), but this shock absorption effect in the midstance phase is not observed when the sole is thicker (Fig. 4-12 and Fig. 4-13). From these results it can be inferred that the toe movement inside a thick sole shoe does not affect the forces between the foot and the ground, making this kind of movement meaningless in terms of shock absorption. This could be one cause of ligament laxity of the plantar area since the outputted motor command has no significant feedback, it will eventually become degraded.

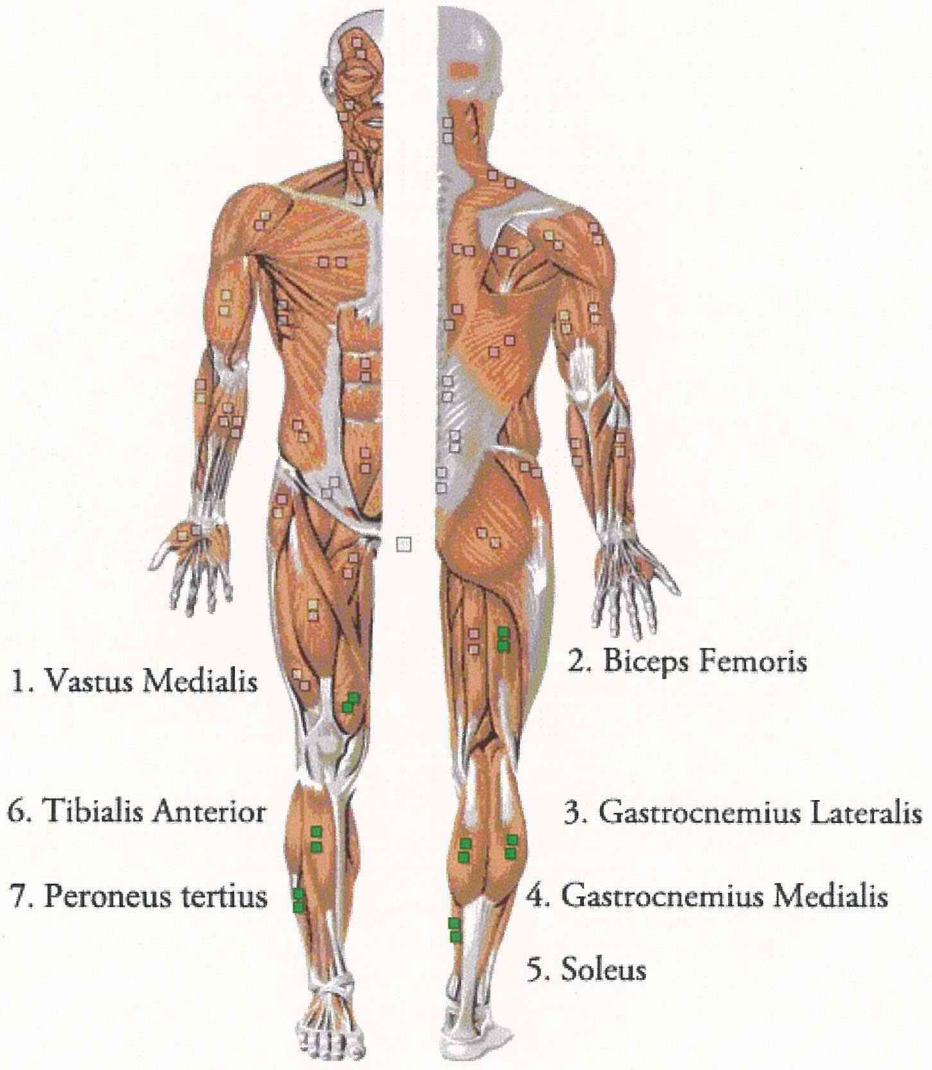

Figure 4-5: EMG electrode placement area

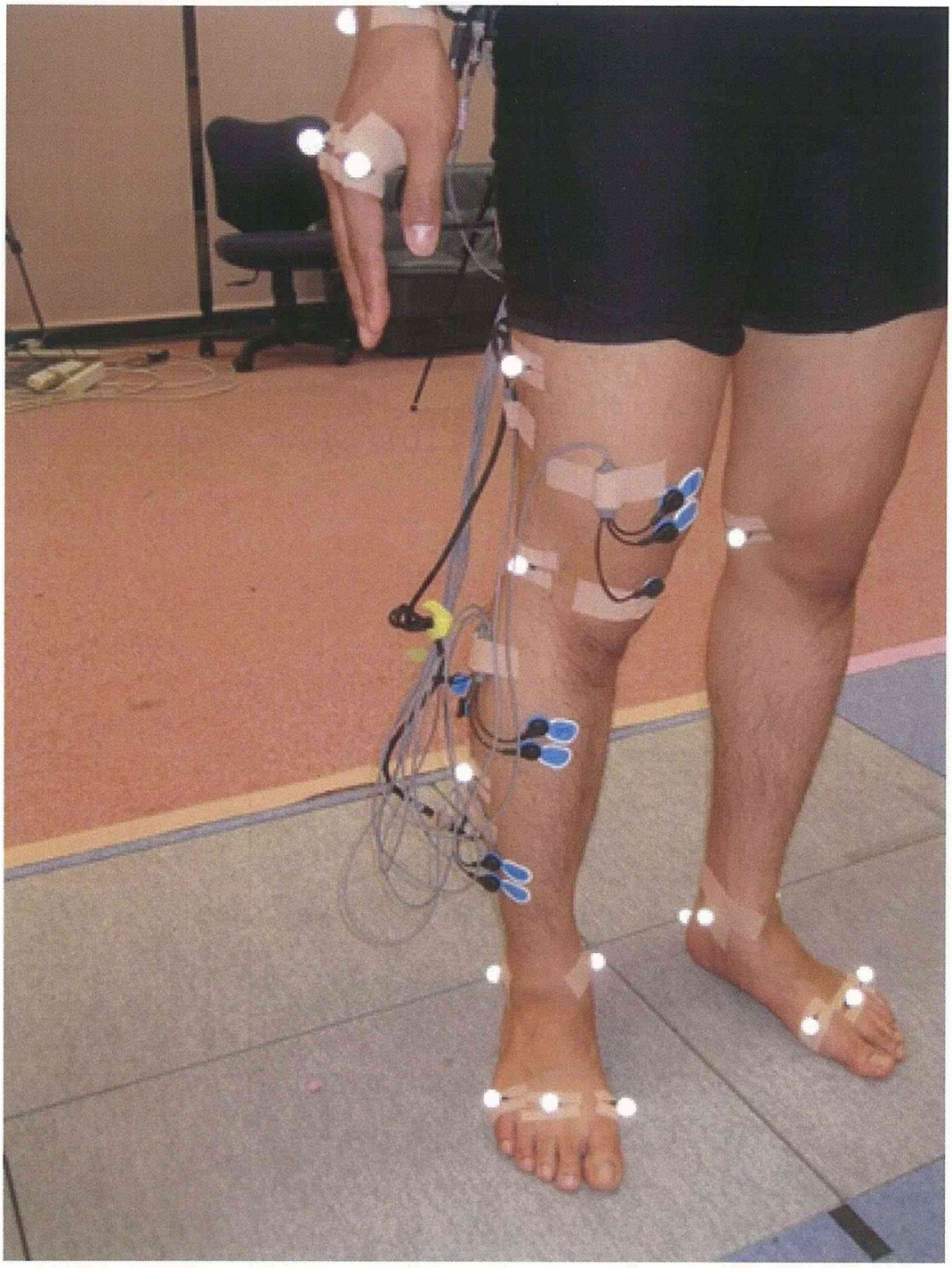

Figure 4-6: EMG electrodes and reflective markers

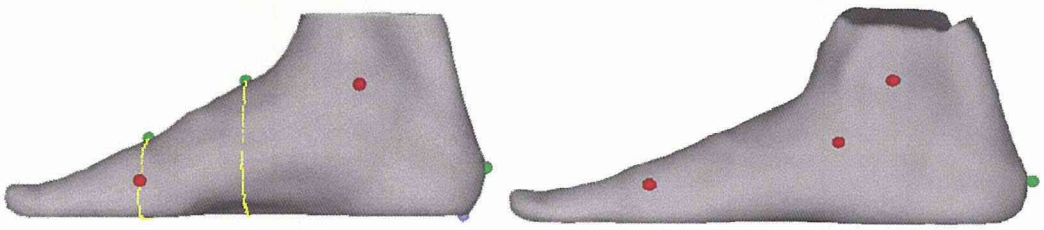

Figure 4-7: Foot shape measured by 3D foot scanner Infoot. High foot arch (Sub A, left) and low foot arch (Sub B, right)

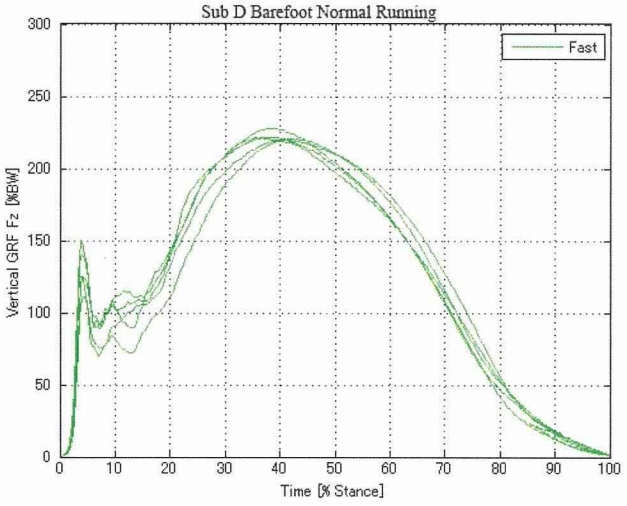

Figure 4-8: Vertical GRF of normal barefoot run

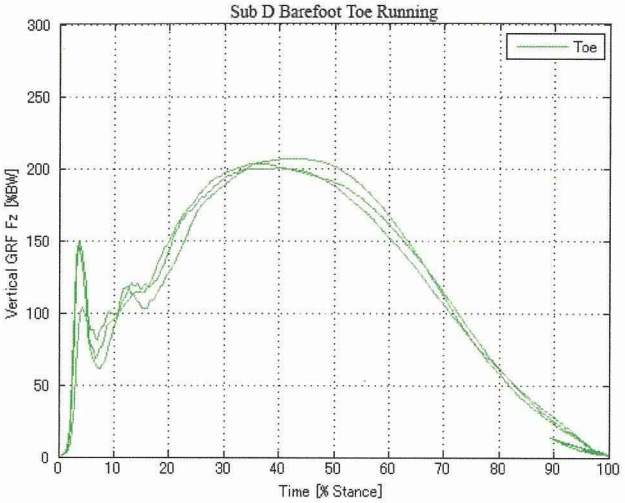

Figure 4-9: Vertical GRF of toe barefoot run

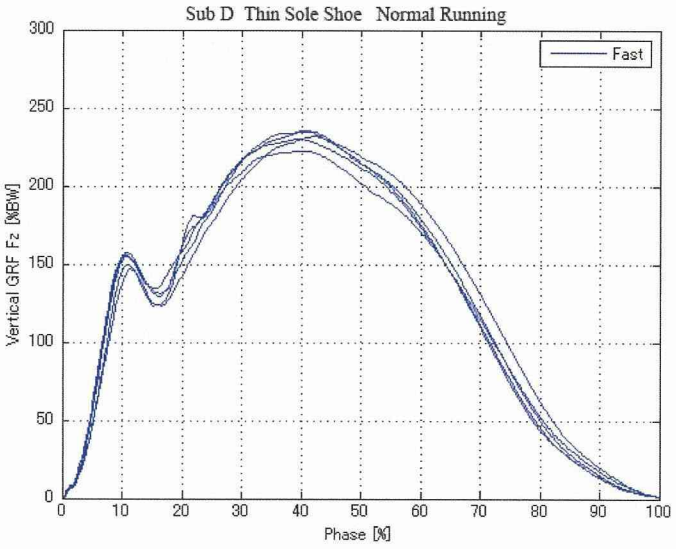

Figure 4-10: Vertical GRF of normal shod run (thin sole)

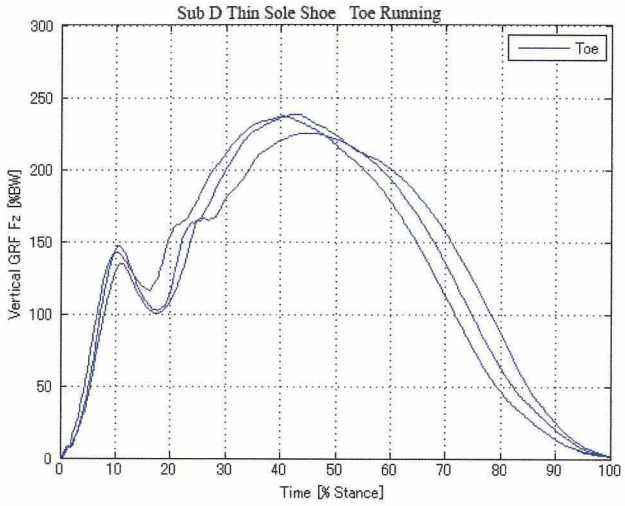

Figure 4-11: Vertical GRF of toe shod run (thin sole)

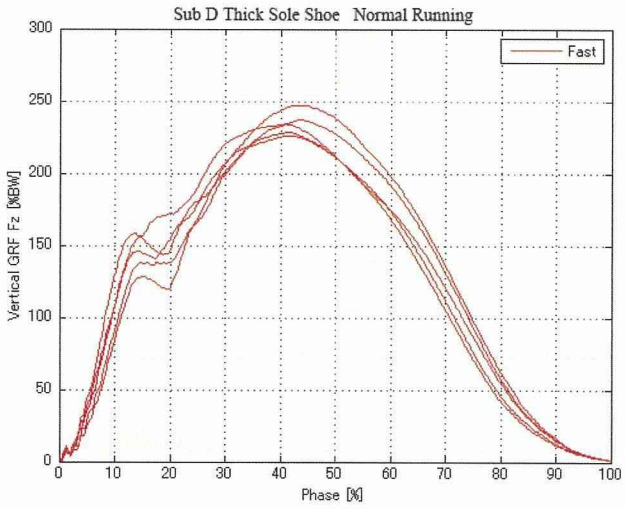

Figure 4-12: Vertical GRF of normal shod run (thick sole)

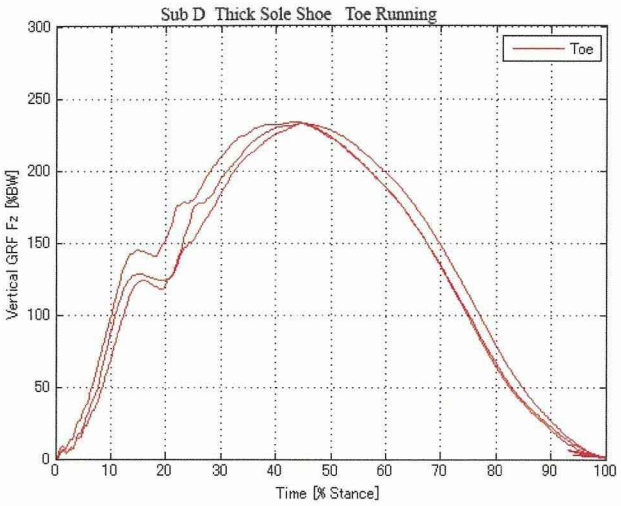

Figure 4-13: Vertical GRF of toe shod run (thick sole)

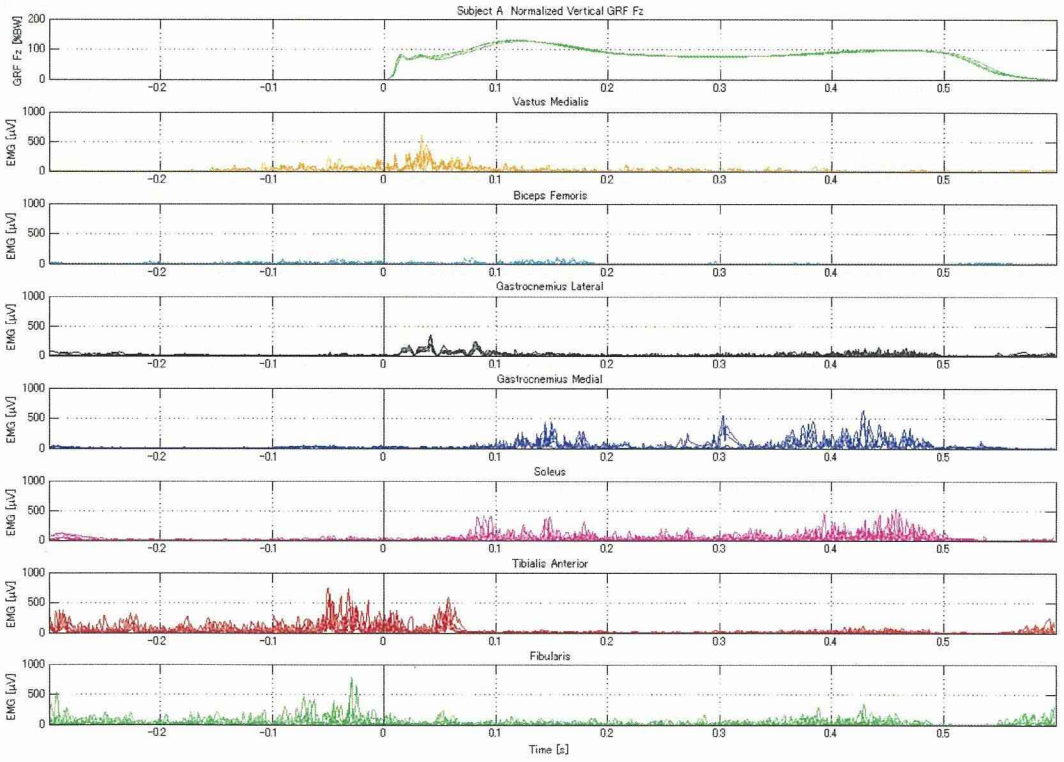

Figure 4-14: GRF and EMG during normal barefoot gait (Sub A)

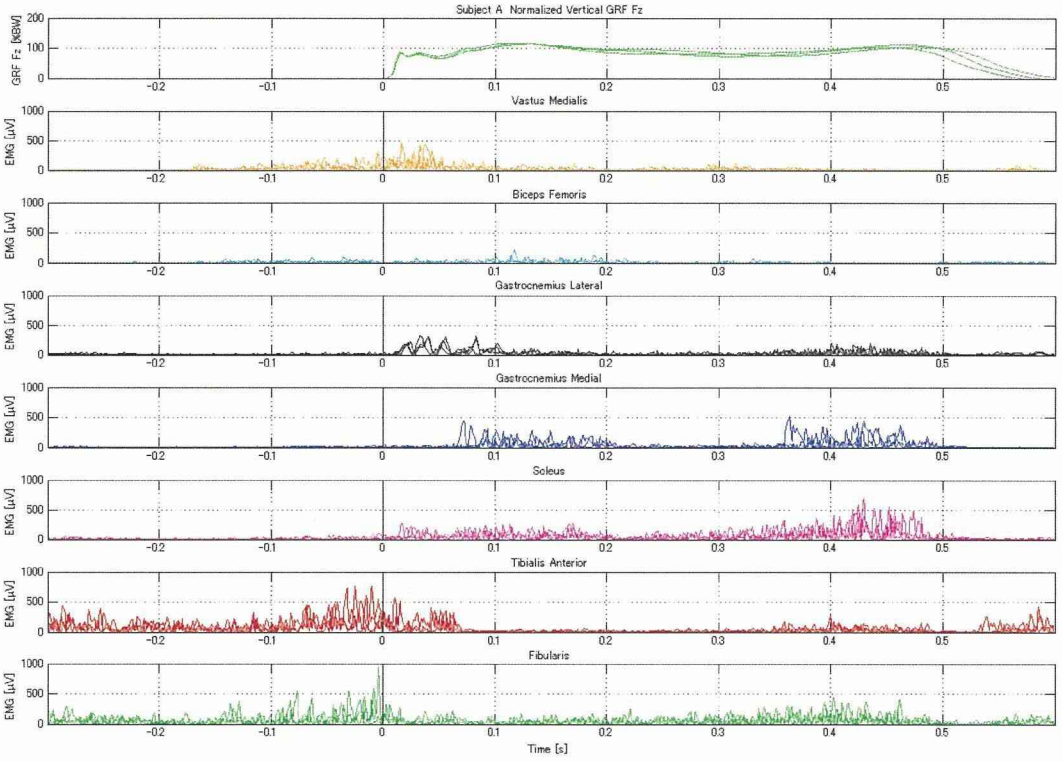

Figure 4-15: GRF and EMG during toe barefoot gait (Sub A)

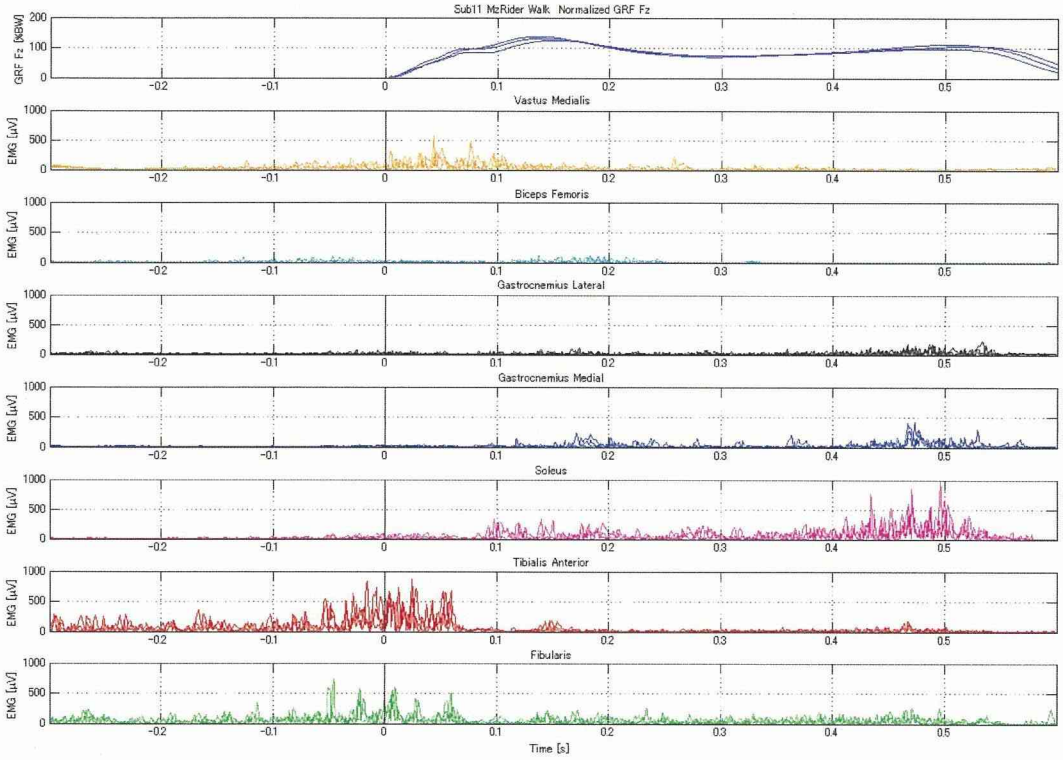

Figure 4-16: GRF and EMG during normal shod gait (Sub A) XXX

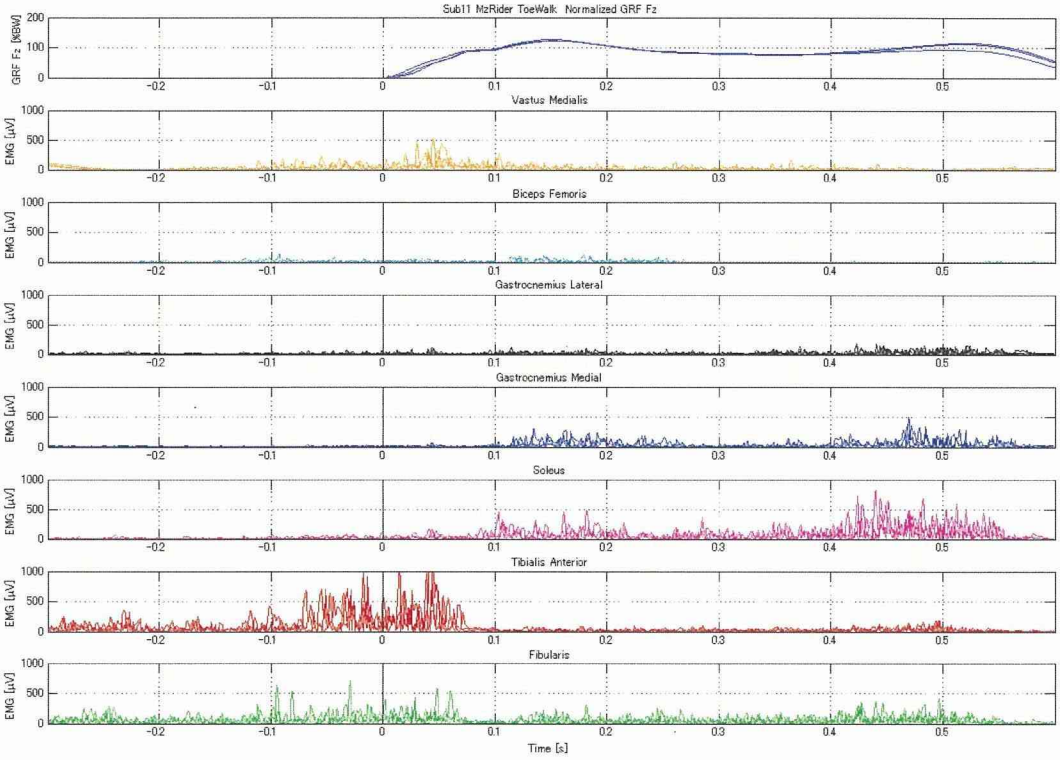

Figure 4-17: GRF and EMG during toe shod gait (Sub A)

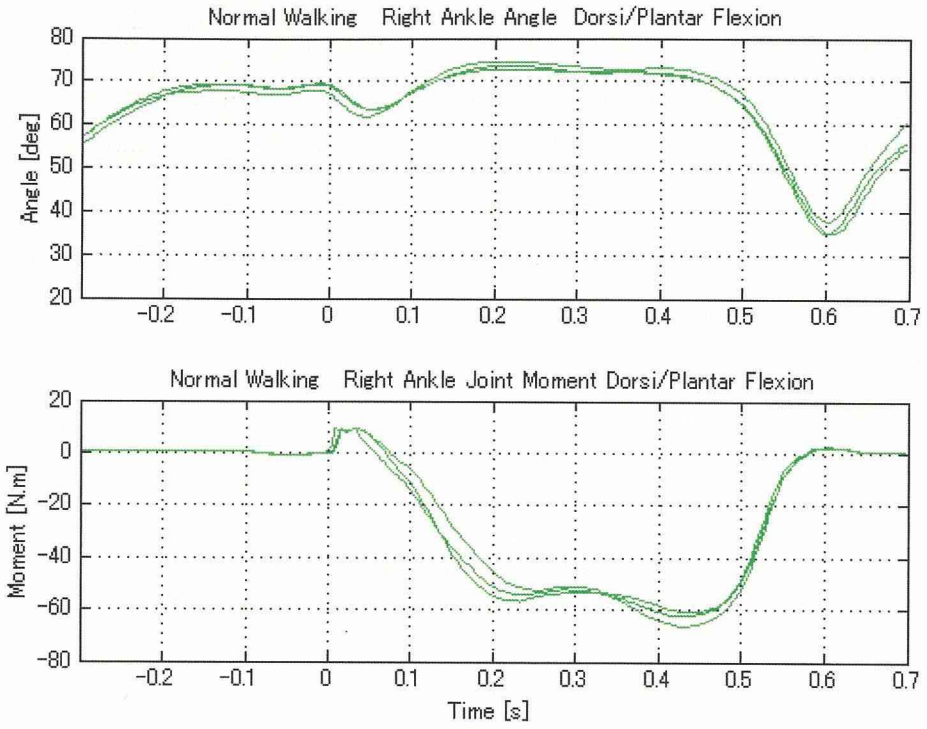

Figure 4-18: Ankle angle and moment during normal barefoot gait (Sub A)

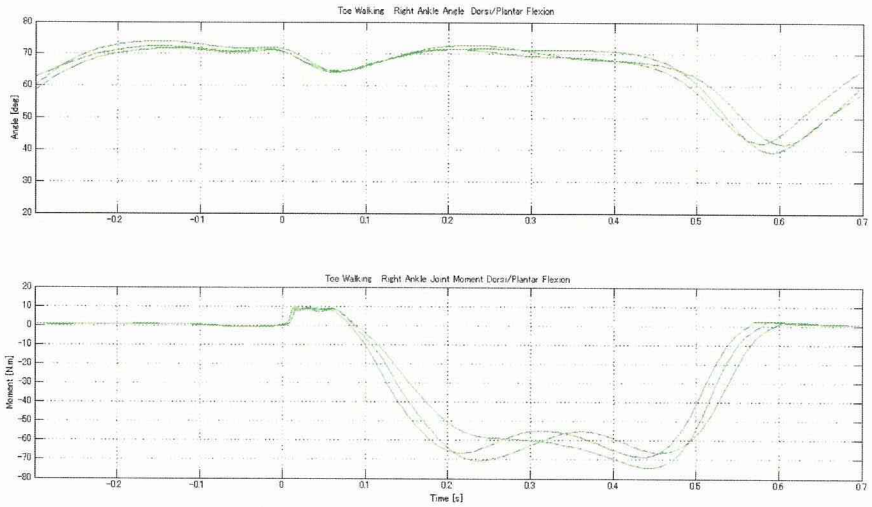

Figure 4-19: Ankle angle and moment during toe barefoot gait (Sub A)

4.3.2 IEMG

The integral of the EMG of each interval was calculated. The EMG signal was rectified, filtered and integrated for each interval. The filter used was a second order Butterworth with a cutoff frequency of 3Hz. The IEMG was calculated in three different phases: Before Heel Contact, Around Heel Contact and After Heel Contact. Different time intervals around and after heel contact were selected depending of the walking/running velocity. The time interval before heel contact was maintained the same because raw EMG signals showed similar initial activation independently of the walking/running speed.

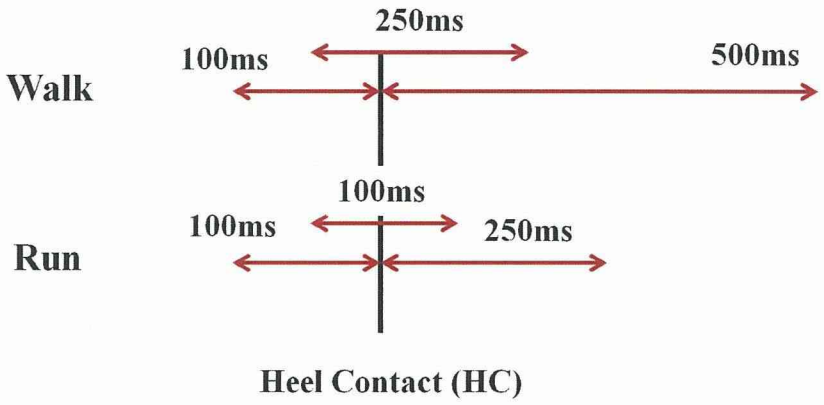

Figure 4-20: Calculation of IEMG of each interval

4.3.3 Dorsi and Plantar Flexion EMG

In order to analyze the toe movement and the motor control strategy the surface EMG of the right leg was measured (See Fig. 4-5 for electrode location). The GRF and the EMG during gait are shown in Fig. 4-14, Fig. 4-15, Fig. 4-16, Fig. 4-17. The 0s time corresponds to the heel contact (HC) and the horizontal axis starts at 0.3s before HC and ends at 0.7s after HC. The vertical axis of the GRF is represented in percentage of body weight (BW).The GRF profile is similar to the previous section with an attenuation of the first peak caused by the thick sole. The maximum voluntary

contraction (MVC) was measured but here the EMG signals are shown in raw value because it will be used in the future to estimate the ankle joint torque. This will be explained in detail in the discussion session. The most prominent difference related to the EMG when moving the toe is the preactivation of plantar flexion muscles (GL, GM, SO) (Compare Fig. 4-14 and Fig. 4-15). When the subject intentionally moved his toe during walking, there is a clear earlier activation in the GL, GM and SO muscles compared to normal walking.

On the other hand, when the toe walking is conducted using thick sole shoe, this preactivation is not so clear but the amplitude seems to increase (Fig. 4-16 and Fig. 4-17). This increase in the EMG amplitude may cause changes in the of ankle joint torque. The change in the ankle joint torque can be verified comparing the graphs in Fig. 4-18 and Fig. 4-19. The toe movement caused an ankle joint torque to increase about 20% in the midstance phase compared to the normal gait. The kinematic and kinetic information were computed using Visual 3D software. However like others 3D motion modeling software it is not possible to compute the co-contraction situation where agonist and antagonist muscles act simultaneously. In order to have more detailed information about the ankle joint stiffness and torque, an estimation method based on EMG signals will be used in this study.

4.3.4 IEMG Statistical Analysis

The statistical analysis results of 3 subjects are shown in Fig. 4-21, Fig. 4-23,Fig. 4-25. The IEMG t-test of walk and run trials related to barefoot and shod condition were conducted in respect to 3 intervals (Before HC, Around HC and After HC). The results showed different behavior depending on the subject. Here $*p < 0.05$ and $**p < 0.01$.

Sub01

Fig. 4-21 shows the result of Sub01 IEMG statistical analysis. According to Fig. 4-21 it can be noticed that only the Around HC interval indicated a statistical difference

between the IEMGs. The only exception was the shod walk/run where no difference was found between normal and toe trials. It means that during shod walk/run the movement of the toes did not have much influence in the IEMG values. Only during barefoot walk/run the movement of the toes was followed by a greater activity in the muscles (Fig. 4-22). Because the IEMG of Around HC interval during shod walk/run was smaller compared to barefoot walk/run, it can be inferred that the use of shoe leads to a decrease in muscle activities.

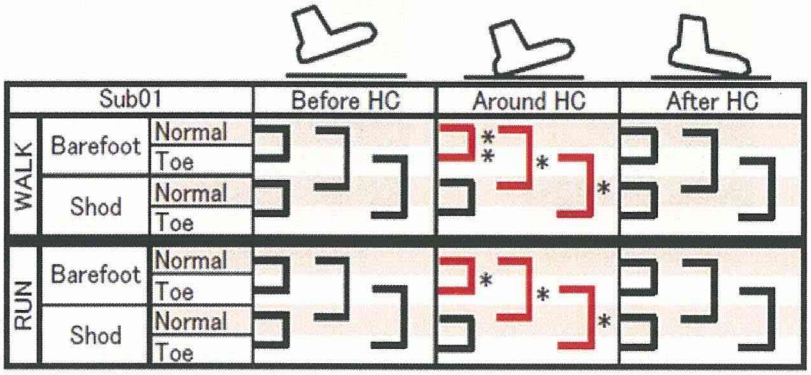

Figure 4-21: Statistical analysis of IEMG of all trial mode (Sub 01)

Sub04

Fig. 4-23 shows the result of Sub04 IEMG statistical analysis. The use of shoe or the movement of the toes did not have much influence over the muscles activities of Sub04. The only statistical difference was found between barefoot and shod walk using the toe during the After HC interval. In this case the shod walk showed a smaller IEMG value compared to barefoot walk. (Fig. 4-24) It seems that the use of shoe or moving the toe do not have much influence in the muscles activities of Sub04.

Sub14

Fig. 4-25 shows the result of Sub14 IEMG statistical analysis. During barefoot and shod walk there was a significant difference between all the intervals (Before HC,

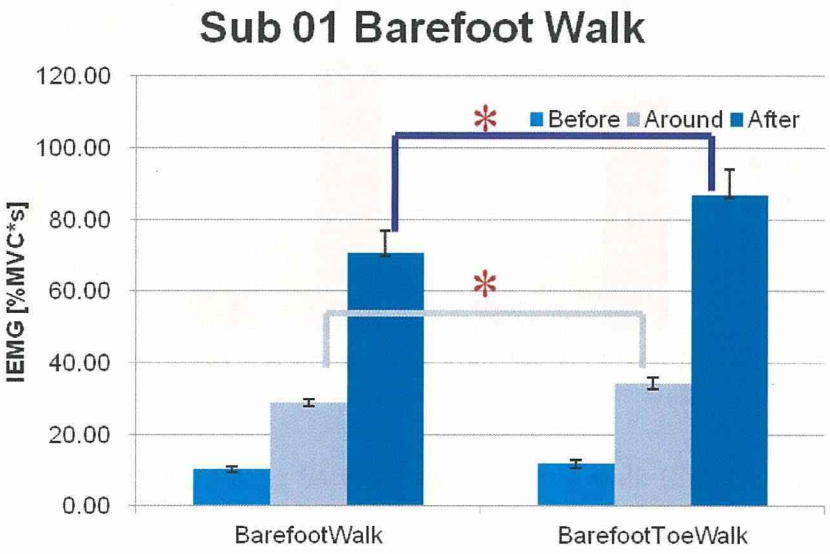

Figure 4-22: IEMG during barefoot walking (Sub 01) $*p < 0.05$

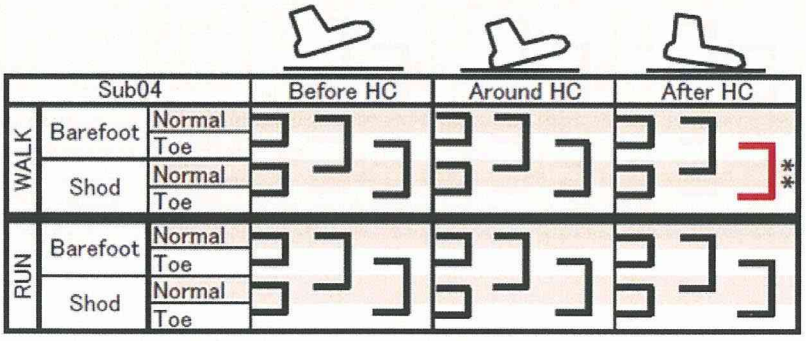

Figure 4-23: Statistical analysis of IEMG of all trial mode (Sub 04)

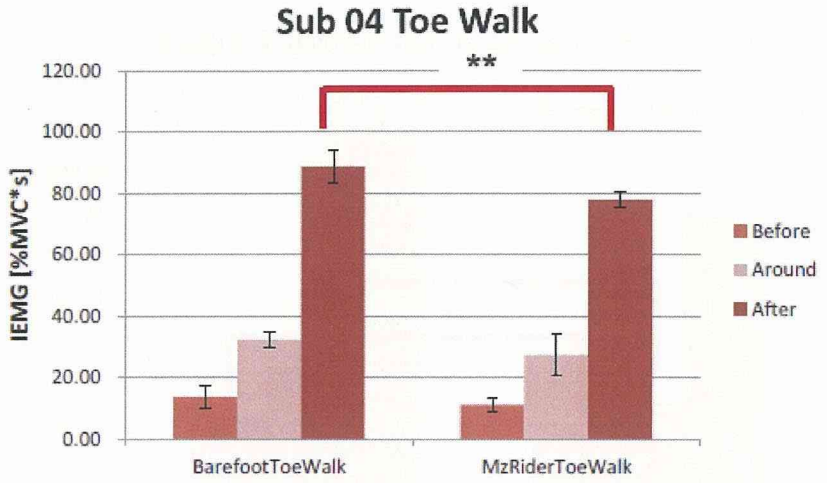

Figure 4-24: IEMG during barefoot and shod toe walk (Sub 04) $*p < 0.05$

Around HC and After HC). On the other hand, during barefoot and shod running using the toe, no difference was found in the IEMG. The only exception was during barefoot running in Before HC and Around HC intervals when the use of toe had influenced the muscles activities.

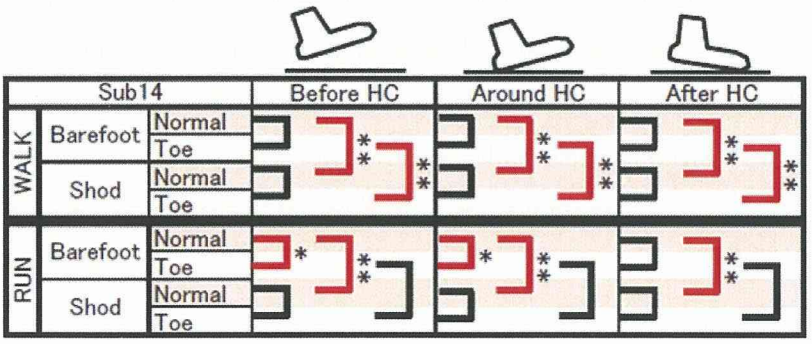

Figure 4-25: Statistical analysis of IEMG of all trial mode (Sub 14)

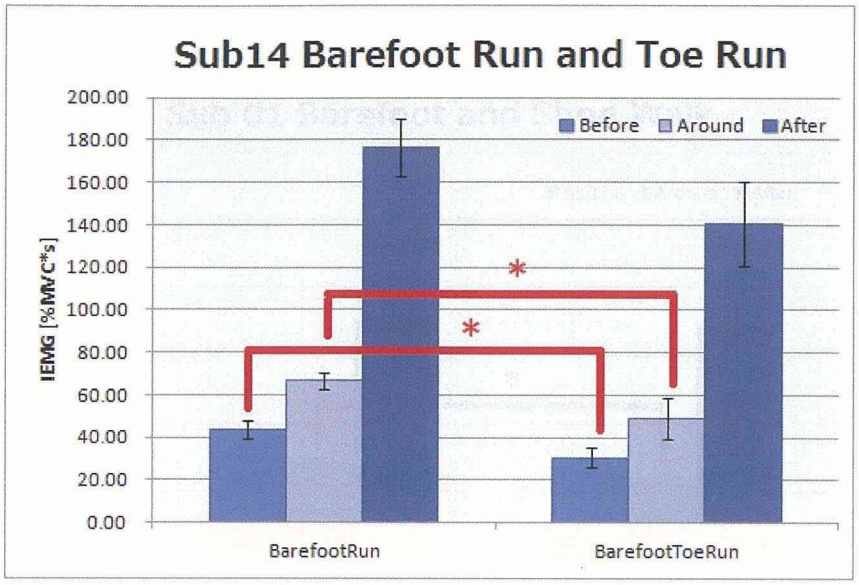

Figure 4-26: IEMG during barefoot normal and toe running (Sub 14) $**p < 0.01$

Discussion

The 3 subjects analyzed showed different characteristics in respect to the muscles activities during barefoot and walk/run using or not the toe. However, when statistical difference between barefoot and shod walk/run existed, all the subjects showed a decrease in the muscle activity during shod walk/run (Fig. 4-27, Fig. 4-28, Fig. 4-29, Fig. 4-29). Because Sub01 showed some statistical difference in muscle activity in Around HC interval during shod walk/run or when using the toe, it can be inferred that he was more concentrated in the heel contact instant.

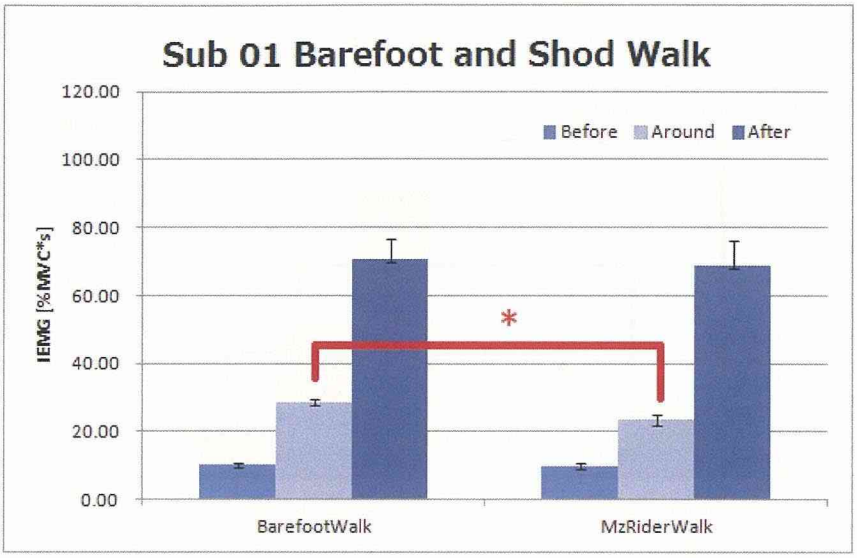

Figure 4-27: IEMG during barefoot and shod walking (Sub 01) $*p < 0.05$

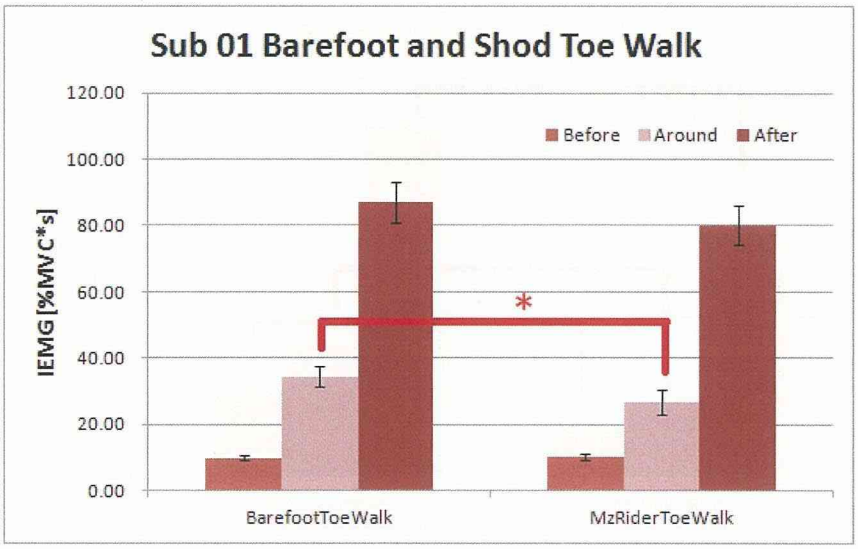

Figure 4-28: IEMG during barefoot and shod toe walking (Sub 01) $*p < 0.05$

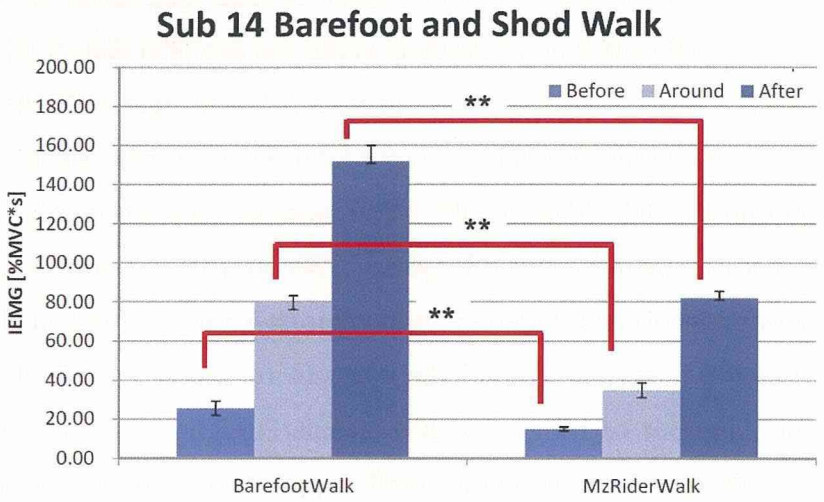

Figure 4-29: IEMG during normal barefoot and shod walking (Sub 14) $**p < 0.01$

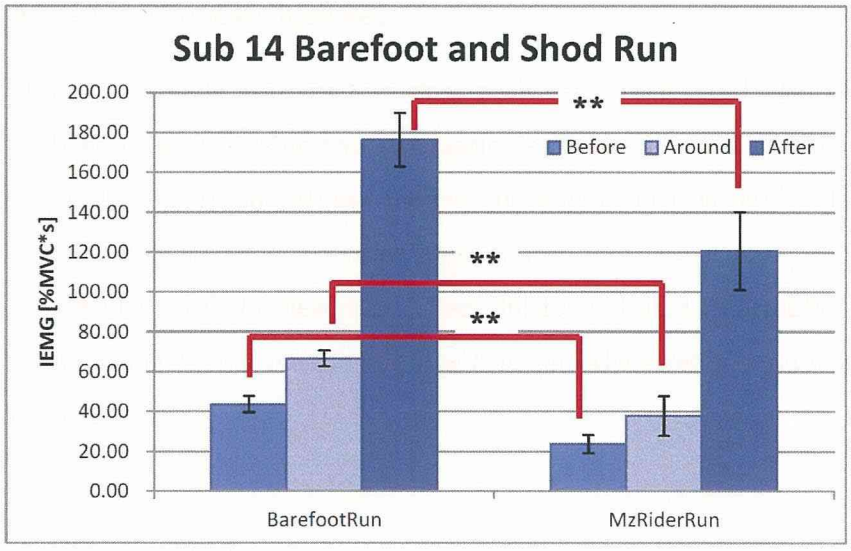

Figure 4-30: IEMG during normal barefoot and shod running (Sub 14) $**p < 0.01$

4.4 Discussion

Previous study using GRF data to analyzed barefoot and shod walking/running was conducted [3] [1] [22] [13], but not many discussion about the effects of toe movement were covered. Although it is not easy to verify the toe movement inside the shoe, the EMG signals offer valuable information about the muscle activity, which can be used to infer about the toe movement. The available 3D motion modelling and biomechanical analysis software offers variety of information about the motion but to understand the motion control strategy in more detail, additional information about the joint stiffness and torque are also needed. Here, a method of estimating the joint torque and stiffness from EMG signals will be applied to the ankle joint. It was originally proposed to estimate upper limb torque and stiffness. The estimation of the ankle joint torque by using the EMG offers the also possibility of measuring the gait and running at more natural conditions like outside activities. If the ankle joint angle can be measured with the EMG signals, the GRF can also be estimated. Next the estimation method will be explained.

4.4.1 Mykin Muscle Model

This model was originally proposed to deal with arm model and also others arm models have been proposed using two kinematic degrees of freedom in the horizontal plane [21] [6] [17] [30]. In the Mykin model, the human arm is modeled as a two-link manipulator with six monoarticular muscles and two biarticular muscles. Here only the main feature will be described. See [36] for detailed information. Muscle tension T is determined from muscle stiffness $k(u)$ and the stretch length of a muscle $[l_r(u) - l(\theta)]$ as follows.

$$T = k(u)[l_r(u) - l(\theta)]$$

$$\begin{cases} k(u) = k_0 + k_1 u \\ l_r(u) = L_{bias} - \Delta L_{eq} = L_{bias} - [L_{eq}(0) - L_{eq}(u)] \\ = L^*_{bias} + L_{eq} u = l_0 + l_1 u \\ l(\theta) = L(0) - L(\theta) \cong \mathrm{A}^{\mathrm{T}}\theta \end{cases} \tag{4.1}$$

see Eq.(4.1)

Here, the parameters k_0 and k_1 of the muscle stiffness $k(u)$ are the intrinsic elasticity and the elasticity, respectively. The muscle stiffness $k(u)$ is represented by linear functions of muscle activation u. $l_r(u)$ denotes the deviation of equilibrium length. It is assumed that can be contracted by only the muscle activation u . L_{bias} represents a bias term and L_{eq} is the deviation of equilibrium length between the equilibrium length $L_{eq}(0)$ and the current equilibrium length $L_{eq}(u)$. L^*_{bias} denotes a bias term that is set so that $[l_r(u) - l(\theta)]$ is not negative. The constant parameter l_0 is the intrinsic rest length when u is zero. $l(\theta)$ denotes the current muscle length with the current joint angle . $L(0)$ denotes the muscle length when the joint angle is 0 and $L(\theta)$ denotes the current muscle length at the current joint angle. It can be simplified as arc $(A^T\theta)$. The lengths value will be referred to previous studies. The others model parameters will be calculated using measured joint angles, torques and EMG signals. The validation of the model will be based on Visual3D output, GRF data and other previous studies [2] [12]. The advantage of Mykin model usage is that it can estimate also co-contraction activities.

4.5 Conclusion

The results of this primary measurement about the effects of toe movement in barefoot and shod walking/running will be used to establish an evaluation method to assess the performance of the two groups. It was observed that even in very short period of time the subject is able to adapt his gait/run pattern to accomplish the determined task. This fast adaptation can be observed by different GRF and EMG profiles. The toe movement showed to be a potential way of changing in an active manner the

characteristics of shock absorption. On the other hand from the results achieved there is a great possibility that this toe movement is impaired by thick sole shoe. The analysis of the ankle joint torque estimation is being conducted with the cooperation of the Mykin model author and the results are expected to be reported in near future.

4.6 Acknowledgement

Part of this work was supported by Mizuno Co., Ltd..

Chapter 5

HUMAN MOTOR LEARNING AND ADAPTATION

It was shown in chapter 3 and chapter 4, respectively, the results of the human control model estimation and the walking/running motion with different shoes. It was acceptable to postulate from these both studies, a scheme to differentiate learning and adaptation related to continuous control task and walking/running motions.

The proposed scheme of learning/adaptation is explained in Fig. (5-1). During our infant phase we learn how to move our body according to a designed goal and/or trajectory. The improvement of our movements is based on continuous adjustment of learned motions. After learning innumerous types of motions and obtained the capability to adapt to new environment, it is not so difficult to perform new tasks. On the other hand this adaptation capability varies from individual to individual, which sometimes can expand to a new learning module. Per example, in the walking/running motions with different shoes, the Sub 01 was able to formulate two different motion patterns when using shoes and when he was in bare feet (Fig. 4-27, Fig. 4-28). In the case of Sub 04, there was no significant difference between his walking/running patterns in terms of EMG when in shod and in bare feet task.

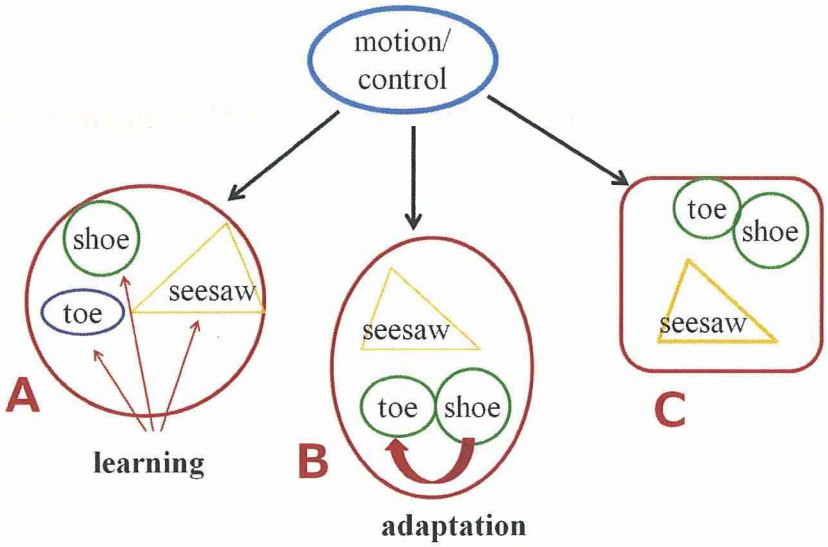

Figure 5-1: Learning and Adaptation Scheme

5.0.1 Human Control Model

In the human control model estimation experiments it was found that the human operator is able to change his control characteristics in order to operate different machines. Here, the training process resulted in different transfer function which represented the learned control model. The parameter of this learned control model differs from subject to subject but the order of the transfer function is assumed to be the same. When the force feedback information was available to the subject, there was a variation in the parameters but the transfer function order was kept the same. So it can be inferred that the subject made some adjustment to deal with the different sensory feedback information provided by the haptic device. Even though the transfer function and also the parameters identified in these experiments are task specific, a common tendency was found related to the subject ' s characteristics. The subject B showed the longest reaction time and also bigger compensation parameter compared to others subjects.

Learning⇒ Different Transfer Function Order

Adaptation⇒ Parameter Adjustment

Figure 5-2: Learning and Adaptation in Human Control Theory

Experiment	Subject A	Subject B	Subject C
Pursuit $H_p(s)$	$\frac{2.3}{1+0.4s}e^{-0.20s}$	$\frac{2.1}{1+0.6s}e^{-0.27s}$	$\frac{2.2}{1+0.5s}e^{-0.22s}$
Visual $H_v(s)$	$6\frac{1+4s}{1+0.06s}e^{-0.24s}$	$4\frac{1+4s}{1+0.2s}e^{-0.31s}$	$10\frac{1+2s}{1+0.03s}e^{-0.21s}$
Visual/Force $H_{vf}(s)$	$10\frac{1+2s}{1+0.04s}e^{-0.23s}$	$8\frac{1+2s}{1+0.1s}e^{-0.29s}$	$13\frac{1+2s}{1+0.04s}e^{-0.22s}$

Figure 5-3: Human Transfer Function: learning case

Experiment	Subject A	Subject B	Subject C
Pursuit $H_p(s)$	$\frac{2.3}{1+0.4s}e^{-0.20s}$	$\frac{2.1}{1+0.6s}e^{-0.27s}$	$\frac{2.2}{1+0.5s}e^{-0.22s}$
Visual $H_v(s)$	$6\frac{1+4s}{1+0.06s}e^{-0.24s}$	$4\frac{1+4s}{1+0.2s}e^{-0.31s}$	$10\frac{1+2s}{1+0.03s}e^{-0.21s}$
Visual/Force $H_{vf}(s)$	$10\frac{1+2s}{1+0.04s}e^{-0.23s}$	$8\frac{1+2s}{1+0.1s}e^{-0.29s}$	$13\frac{1+2s}{1+0.04s}e^{-0.22s}$

Figure 5-4: Human Transfer Function: adaptation case

5.0.2 Walking and Running Analysis

The IEMG statistical analysis results of the walking and running experiments showed that depending on the subject different muscle activation strategy was selected (Fig. 4-21, Fig. 4-23, Fig. 4-25). In the case of Sub01 not only the IEMG (Fig. 5-6) showed a statistical difference but also the ground reaction force (GRF). The first peak in Fig. 5-5 and Fig. 5-7 shows the ground reaction force between the heel contact and the flat foot instant. In Fig. 5-5 a significant difference in the maximum GRF between normal and toe barefoot running is shown (Sub01). From these results it can be inferred that when a significant difference exists, the subject was able to perform distinct muscle motor activation patterns.

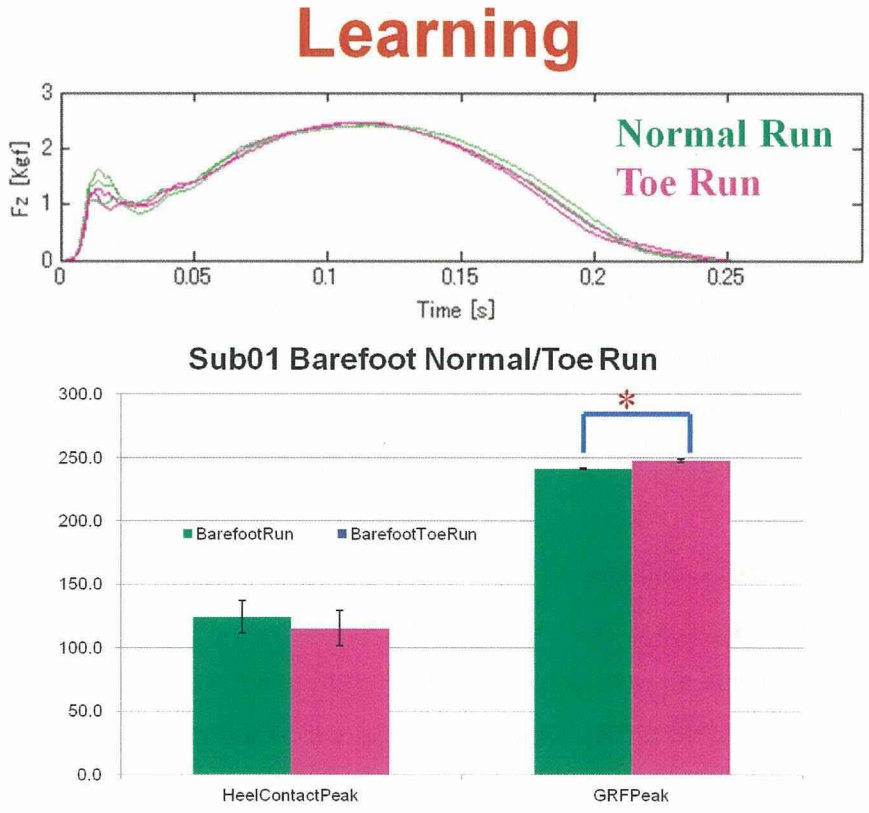

Figure 5-5: Walking/Running study: learning case

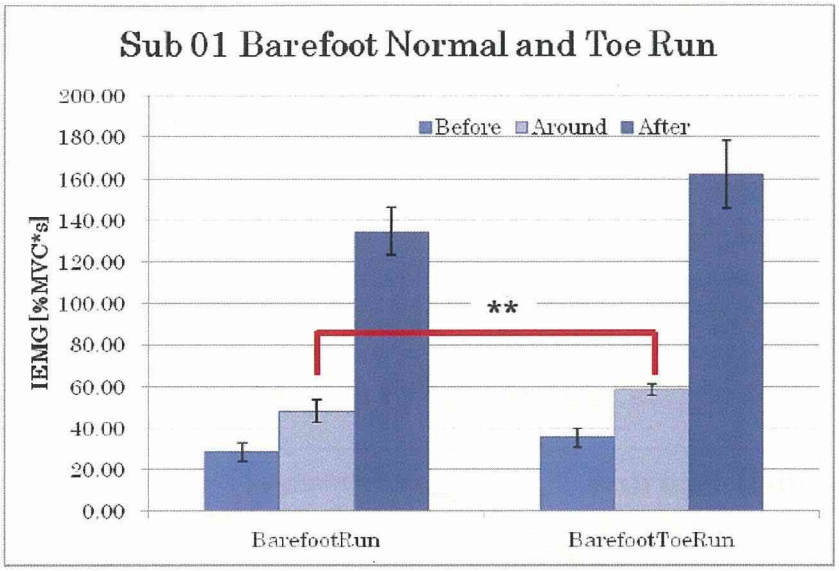

Figure 5-6: IEMG during barefoot running (Sub 01) $*p < 0.05$

On the other hand, since no significant statistical difference was found between the IEMG intervals (Fig. 5-8), it can be inferred that the subject was not capable to perform different motion patterns. As it shown in Fig. 5-7 the similar behavior of the Sub01 in terms ground reaction force also illustrated the same indifference of muscle activation, represented by the IEMG of normal and toe run in shod condition. Moreover in the case of Sub04, there was almost no difference between any combination of trials including the comparison barefoot/shod and normal/toe walk and run experiments (Fig. 4-23).

From these two different characteristics it can be concluded that the use of shoes in some way inhibited the learning of a new motor control strategy. This can be one of the causes why the prolonged use of shoe changed how we strike the ground and consequently caused the relaxation of the plantaris muscles [31].

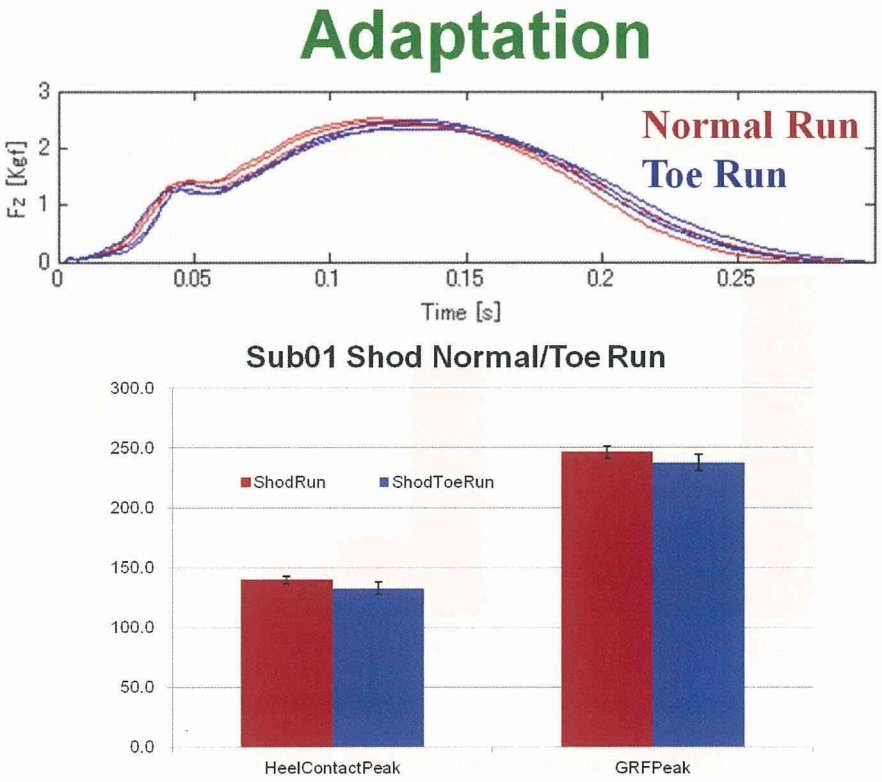

Figure 5-7: Walking/Running study:: adaptation case

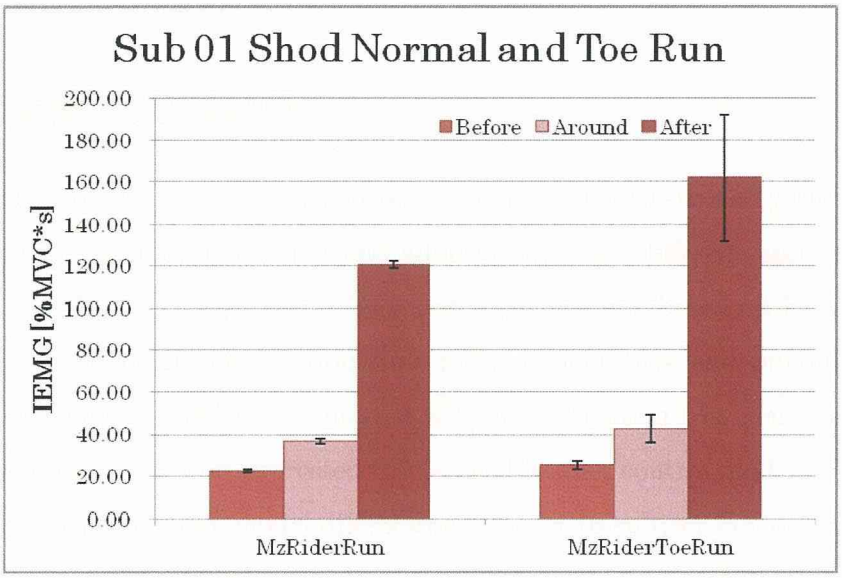

Figure 5-8: IEMG during shod running (Sub 01) $*p < 0.05$

Chapter 6

FINAL CHAPTER

6.1 DISCUSSION

The objective of this research was to represent in a quantitative way the difference between the terms motor learning and adaptation. Two different approaches were selected to deal with this problem. The first approach was based on human control model identification during reaction time measurement task and pursuit tracking. The human control model represented as a transfer function was identified and the estimated transfer function expressed the learned human control model. The parameter of this learned control model differs from subject to subject but the order of the transfer function is assumed to be the same. When the force feedback information was available to the subject, there was a variation in the parameters but the transfer function order was kept the same. So it can be inferred that the subject made some adjustment to deal with the different sensory feedback information provided by the haptic device. Furthermore, the difference in the order of the transfer functions when manipulating various machine characteristics represented the learned control model. On the other side small variation in the parameters due to the presence of different sensory information can be correlated to the subject's capability of adaptation. The second approach was based on walking and running motion when using different shoe sole thickness. The results of the walking and running analysis showed that depending on the subject different muscle activation strategy was selected. When there was a

significant difference between normal and toe barefoot running it can be inferred that the subject was able to perform two distinct muscle motor activation. On the other hand, when no significant difference difference between the IEMG of the normal and toe run using shoes occurred it can be inferred that similar behaviour of the subject in terms of muscle activation took place.

The two approaches, transfer function modeling and IEMG statistical analysis, adopted here appears to have no relation with each other. But in fact, if the body dynamics during walk/run task can be modeled using transfer function, the function order and the parameters can also be used to explain the learning and adaptation strategies.

6.2 CONCLUSION

The two approaches chosen in this study to analyze the motor learning and adaptation was shown to be promising way to understand how the learning and adaptation occurs in various types of motions. The direct measurement of the reaction time using also EMG signals gave insights about the individual variation between subjects showing that the EMG-RT time was responsible for such difference. This measured reaction time was also correlated to the time delay estimated from continuous pursuit tracking task. It was shown that the human acquired model depended on the machine characteristics and the learned model was associated with the transfer function order. When different sensorial information was available to the subjects, there were noted small variations in the transfer function parameters representing the subjects capability to adapt to different sensorial feedback information. In the walking and running experiment it was observed that even in very short period of time the subject was able to adapt his gait/run pattern to accomplish the determined task. This fast adaptation can be observed by different GRF and EMG profiles. The toe movement showed to be a potential way of changing in an active manner the characteristics of shock absorption. On the other hand from the results achieved there is a great possibility that this toe movement is impaired by thick sole shoe. Because there were no much change in the subject's behaviour between normal and toe running when using

shoe, it can be presumed that the use of shoes in some way inhibited the learning of a new motor control strategy. This can be one of the causes why the prolonged use of shoe changed how we strike the ground and consequently caused the relaxation of the plantaris muscles.

Appendix A

Tables

Table A.1: SRT Experiment - EMG Activation and Onset Time

Experiment	Subject A	Subject B	Subject C
Onset [s]	0.21 ± 0.03	0.26 ± 0.04	0.20 ± 0.03
EMG-RT[s]	0.19 ± 0.04	0.21 ± 0.04	0.15 ± 0.03
EMD [s]	0.03 ± 0.02	0.05 ± 0.01	0.05 ± 0.01

Table A.2: CRT Experiment - EMG Activation and Onset Time

Experiment	Subject A	Subject B	Subject C
Onset [s]	0.24 ± 0.02	0.32 ± 0.05	0.27 ± 0.04
EMG-RT[s]	0.19 ± 0.02	0.28 ± 0.04	0.20 ± 0.04
EMD [s]	0.04 ± 0.01	0.04 ± 0.02	0.06 ± 0.03

Table A.3: Estimation of time lag from step response - SRT

Parameters	Subject A	Subject B	Subject C
ω_n [rad/s]	27 ± 2	15 ± 5	20 ± 2
ζ	0.34 ± 0.04	0.48 ± 0.08	0.50 ± 0.03
τ_d [s]	0.24 ± 0.03	0.29 ± 0.04	0.26 ± 0.03

Table A.4: Estimation of time lag from step response - CRT

Parameters	Subject A	Subject B	Subject C
ω_n [rad/s]	27 ± 2	18 ± 6	18 ± 2
ζ	0.46 ± 0.11	0.40 ± 0.01	0.52 ± 0.06
τ_d [s]	0.28 ± 0.03	0.36 ± 0.05	0.31 ± 0.04

Bibliography

[1] A. Bertani, A. Cappello, MG Benedetti, L. Simoncini, and F. Catani. Flat foot functional evaluation using pattern recognition of ground reaction data. *Clinical Biomechanics*, 14(7):484–493, 1999.

[2] M. Casadio, P.G. Morasso, and V. Sanguineti. Direct measurement of ankle stiffness during quiet standing: implications for control modelling and clinical application. *Gait & posture*, 21(4):410–424, 2005.

[3] P.R. Cavanagh and M.A. Lafortune. Ground reaction forces in distance running. *Journal of Biomechanics*, 13(5):397–406, 1980.

[4] M.A. Conditt, F. Gandolfo, and F.A. Mussa-Ivaldi. The motor system does not learn the dynamics of the arm by rote memorization of past experience. *Journal of Neurophysiology*, 78(1):554, 1997.

[5] N. Deborh A, B. Judith F, and U. Brian R. Relationship between clinical measurements and motion of the first metatarsophalangeal joint during gait. *The Journal of Bone and Joint Surgery (American)*, 81(3):370–6, 1999.

[6] AG Feldman, SV Adamovich, DJ Ostry, and JR Flanagan. The origin of electromyograms-explanations based on the equilibrium point hypothesis. *Multiple muscle systems: Biomechanics and movement organization*, pages 195–213, 1990.

[7] T. Flash and I. Gurevich. Arm stiffness and movement adaptation to external loads. In *Engineering in Medicine and Biology Society, 1991. Vol. 13: 1991.*,

Proceedings of the Annual International Conference of the IEEE, pages 885–886. IEEE, 1992.

[8] D.W. Franklin, E. Burdet, R. Osu, M. Kawato, and T.E. Milner. Functional significance of stiffness in adaptation of multijoint arm movements to stable and unstable dynamics. *Experimental brain research*, 151(2):145–157, 2003.

[9] D.W. Franklin, R. Osu, E. Burdet, M. Kawato, and T.E. Milner. Adaptation to stable and unstable dynamics achieved by combined impedance control and inverse dynamics model. *Journal of neurophysiology*, 90(5):3270–3282, 2003.

[10] D.W. Franklin, U. So, M. Kawato, and T.E. Milner. Impedance control balances stability with metabolically costly muscle activation. *Journal of neurophysiology*, 92(5):3097, 2004.

[11] F. Gandolfo, FA Mussa-Ivaldi, and E. Bizzi. Motor learning by field approximation. *Proceedings of the National Academy of Sciences*, 93(9):3843, 1996.

[12] WF Genadry, RE Kearney, and IW Hunter. Dynamic relationship between emg and torque at the human ankle: variation with contraction level and modulation. *Medical and Biological Engineering and Computing*, 26(5):489–496, 1988.

[13] G. Giakas and V. Baltzopoulos. Time and frequency domain analysis of ground reaction forces during walking: an investigation of variability and symmetry. *Gait & Posture*, 5(3):189–197, 1997.

[14] J. Hecht, YS Abu-Mostafa, D. Psaltis, JL Horner, D. Neher, A. Wolf, C. Bubeck, G. Wegner, R.D. Miller, J. Mich, et al. Computations underlying the execution of movement: A biological perspective. *J. Phys. Chem*, 90:5703, 1986.

[15] N. Hogan. The mechanics of multi-joint posture and movement control. *Biological cybernetics*, 52(5):315–331, 1985.

[16] A. Kadiallah, G. Liaw, M. Kawato, D.W. Franklin, and E. Burdet. Impedance control is selectively tuned to multiple directions of movement. *Journal of Neurophysiology*, 2011.

[17] M. Katayama and M. Kawato. Virtual trajectory and stiffness ellipse during multijoint arm movement predicted by neural inverse models. *Biological Cybernetics*, 69(5):353–362, 1993.

[18] M. Kawato. Internal models for motor control and trajectory planning. *Current opinion in neurobiology*, 9(6):718–727, 1999.

[19] M. Kawato and H. Gomi. A computational model of four regions of the cerebellum based on feedback-error learning. *Biological cybernetics*, 68(2):95–103, 1992.

[20] Tomohiro Kizuka, Takaai Asami, and Kasunori Tani. Relationship between the degree of inhibited stretch reflex activities of the wrist flexor and reaction time during quick extension movements. *Electroencephalography and Clinical Neurophysiology/Electromyography and Motor Control*, 105(4):302–308, August 1997.

[21] Y. Koike and M. Kawato. Estimation of dynamic joint torques and trajectory formation from surface electromyography signals using a neural network model. *Biological Cybernetics*, 73(4):291–300, 1995.

[22] D.E. Lieberman, M. Venkadesan, W.A. Werbel, A.I. Daoud, S. D ' andrea, I.S. Davis, R.O. Mang ' Eni, and Y. Pitsiladis. Foot strike patterns and collision forces in habitually barefoot versus shod runners. *Nature*, 463(7280):531–535, 2010.

[23] D.T. McRuer, United States. National Aeronautics, Space Administration. Scientific, and Technical Information Program. *Pilot-induced oscillations and human dynamic behavior*, volume 4683. NASA, 1995.

[24] D.T. McRuer and H.R. Jex. A review of quasi-linear pilot models. *Human Factors in Electronics, IEEE Transactions on*, (3):231–249, 1967.

[25] E.A.Y. Murakami, T. Kondo, and K. Ito. Man-machine dynamic characteristics related to position and force control tasks in micro-teleoperation systems. In *SICE 2003 Annual Conference*, volume 2, pages 1620–1625. IEEE, 2003.

[26] E.A.Y. Murakami, K. Shibata, X.Z. Zheng, and K. Ito. Human control characteristics in bilateral micro-teleoperation system. In *Industrial Electronics Society, 2000. IECON 2000. 26th Annual Confjerence of the IEEE*, volume 1, pages 602–607. IEEE, 2000.

[27] Edwardo Arata Y. Murakami, 柴田 克成, 鄭 心知, and 伊藤 宏司. 人間の動作特性を考慮したバイラテラル・マイクロテレオペレーション. **自律分散システム・シンポジウム資料** = *SICE Symposium on Decentralized Autonomous Systems*, 12:447–452, 2000-01-21.

[28] F.A. Mussa-Ivaldi, S.F. Giszter, and E. Bizzi. Linear combinations of primitives in vertebrate motor control. *Proceedings of the National Academy of Sciences*, 91(16):7534, 1994.

[29] R. Osu, D.W. Franklin, H. Kato, H. Gomi, K. Domen, T. Yoshioka, and M. Kawato. Short-and long-term changes in joint co-contraction associated with motor learning as revealed from surface emg. *Journal of neurophysiology*, 88(2):991, 2002.

[30] R. Osu and H. Gomi. Multijoint muscle regulation mechanisms examined by measured human arm stiffness and emg signals. *Journal of neurophysiology*, 81(4):1458, 1999.

[31] U.B. Rao and B. Joseph. The influence of footwear on the prevalence of flat foot. a survey of 2300 children. *Journal of Bone and Joint Surgery-British Volume*, 74(4):525, 1992.

[32] N. Saijo, I. Murakami, S. Nishida, and H. Gomi. Large-field visual motion directly induces an involuntary rapid manual following response. *The Journal of neuroscience*, 25(20):4941–4951, 2005.

[33] RL Sainburg, C. Ghez, and D. Kalakanis. Intersegmental dynamics are controlled by sequential anticipatory, error correction, and postural mechanisms. *Journal of Neurophysiology*, 81(3):1045, 1999.

[34] R. Shadmehr and F.A. Mussa-Ivaldi. Adaptive representation of dynamics during learning of a motor task. *The Journal of Neuroscience*, 14(5):3208–3224, 1994.

[35] T.B. Sheridan. *Telerobotics, automation, and human supervisory control.* The MIT press, 1992.

[36] D. Shin, J. Kim, and Y. Koike. A myokinetic arm model for estimating joint torque and stiffness from emg signals during maintained posture. *Journal of neurophysiology*, 101(1):387–401, 2009.

[37] E. Todorov et al. Direct cortical control of muscle activation in voluntary arm movements: a model. *nature neuroscience*, 3:391–398, 2000.

[38] D.M. Wolpert, K. Doya, and M. Kawato. A unifying computational framework for motor control and social interaction. *Philosophical Transactions of the Royal Society of London. Series B: Biological Sciences*, 358(1431):593–602, 2003.